

[Catégorie]



D1.2: Scientific Requirements Consolidation

Project number

313238

Project title

LOTUS- Preparing Land and Ocean Take Up from Sentinel-3

Call (Part) identifier

FP7-SPACE-2012-1

Reference: CLS-DOS-NT-13-235

Nomenclature: LOTUS-D1.2

Issue: 1. 0

Date: Oct. 20, 13

Funding scheme

Collaborative project

Deliverable Number D1.2

Title: "Minutes of first project meeting."

Nature: Report

Dissemination level: Public





Chronology Issues:			
Issue:	Date:	Reason for change:	Author
1.0	20/10/13	Creation of document Issue 1.0	T. Moreau P. Thibaut
2.0	10/12/13	Update with input from DHI	P.Thibaut, H.Madsen, J.T.Sorensen

People involved in this issue:		
Written by (*):	T. Moreau (CLS) P. Thibaut (CLS), H. Madsen (DHI)	Date + Initials:(visa or ref)
Checked by (*):	AQM	Date + Initial:(visa ou ref)
Approved by (*):	P.Knudsen	Date + Initial:(visa ou ref)
Application authorized by (*):		Date + Initial:(visa ou ref)

**In the opposite box: Last and First name of the person + company if different from CLS*

Index Sheet:	
Context:	
Keywords:	[Mots clés]
Hyperlink:	

Distribution:		
Company	Means of distribution	Names
CLS	Notification	T.Moreau, F.Mercier, P.Thibaut
DTU		P.Knudsen, O.Andersen, K.Nielsen
Starlab		A.Egido, L.Moreno
DHI		H.Madsen, J.T.Sorensen



List of tables and figures

List of tables:

List of figures:

Figure 2.1 Example of wind mill farm in the North Sea that would have benefited from more accurate estimates of high frequent part of the wind sea spectrum.....	5
Figure 3.1 : SLA spectra for Jason 2 data (black), Pseudo-LRM waveforms from Cryosat-2 data (blue), and SAR waveforms from Cryosat-2 data (red). The spectral bump is clearly visible and it is located at spectral wavenumbers between 10 km and 80 km. The spectral bump is totally removed with SAR processing [Thibaut et al., 2013].....	9
Figure 6.1 : SAR echoes simulator [Desjonquères et al., 2012].	17
Figure 6.2 : The resulting weighting function without (top) and after (below) the application of Hamming window in along-track direction	19
Figure 6.3 : Cryosat-2 SAR waveforms over sea ice before (left) and after (right) along-track Hamming weighting (Courtesy Rob Cullen, ESA).....	20
Figure 6.4 : CryoSat-2 AIR with and without Hamming window (zero-padding of 64) [AD3]	20
Figure 6.5 : Antenna gain, DDM, and Doppler echoes representation for an across-track mispointing ($\xi_{ac} = 0.5^\circ$ and $\xi_{al} = 0^\circ$) [Halimi, 2013]	21
Figure 6.6 : Antenna gain, DDM, and Doppler echoes representation for an along-track mispointing ($\xi_{ac} = 0^\circ$ and $\xi_{al} = 0.5^\circ$) [Halimi, 2013]	21
Figure 6.7 : Dependence of the SAMOSA-3 model on (left) along-track and (right) across-track mispointing [Gommenginger et al., 2011].	22
Figure 6.8 : Dependence of the SAMOSA-3 model on Sigma0 [Gommenginger et al., 2011].	22
Figure 6.9 : Square errors calculated for different values of a and b [Boy et al., 2013].....	23
Figure 6.10 : (Right) Figure shows [Galín et al., 2013].....	24
Figure 6.11 : Waveform classification provided in Jason-2 coastal PISTACH products (CNES products) (Thibaut et al, 2010)	25
Figure 6.12 : Location of all data sets selected for the GPD computation: blue - ECMWF grid points over ocean; brown ECMWF grid points over land up to 30 km from the coast; green - Envisat ground track points with valid MWR data; red - Envisat points with invalid MWR data; black - GNSS stations.	27
Figure 6.13 : Location of Envisat cycle 58 ground track points selected for the GPD computation. Only points with invalid MWR data ($MWR_REJ \neq 0$) are shown. Dark green: points with $MWR_REJ=1$; Light green: points with $MWR_REJ=2$; Blue: points with $MWR_REJ=3$; Red: points with $MWR_REJ=4$; Pink: points with $MWR_REJ=5$ (see text for details).	28
Figure 6.14 : Formal error (in metres) for EnviSat cycle 58.	29
Figure 17 : CS-2 LRM/SAR/SARIn mode mask for 3 different periods ..Error! Bookmark not defined.	

Applicable documents

AD 1 CryoSat Products Specification Format, Instrument Processing Facility L1b,
CS-RS-ACS-GS-5106, version 4.9, 14 Nov. 2011



AD 2 CryoSat Products Specification Format, Instrument Processing Facility 2,
CS-RS-ACS-GS-5123, version 2.8, 14 Nov. 2011

AD 3 CryoSat Product Handbook, April 2013

Reference documents

RD 1 CRYOSAT products handbook:

https://earth.esa.int/c/document_library/get_file?folderId=125272&name=DLFE-3605.pdf

**Acronyms List**

AIR	Azimuth Impulse Response
CPP	Cryosat Processing Prototype
DDM	Delay/Doppler Map
EC	European Commission
EO	Earth Observation
ESA	European Space Agency
FSSR	Flat Sea Surface Response
LRM	Low Resolution Mode
LSE	Least Squares Estimator
NA	Not Applicable
NOAA	National Oceanic and Atmospheric Administration
NRT	Near Real Time
PLRM	Pseudo Low Resolution Mode (# RDSAR)
POD	Precise Orbit Determination
PTR	Point Target Response
RD	Reference Document
RDSAR	Reduces Synthetic Aperture radar (# PLRM)
RIR	Range Impulse Response
SAR	Synthetic Aperture radar
SIRAL	Synthetic Aperture Interferometric Radar Altimeter
SLA	Sea level Anomalies
SRAL	SAR Radar Altimeter
SSB	Sea State Bias
SWH	Significant Wave Height



List of Contents

1. Introduction.....	1
1.1. Aim.....	1
1.2. Document content	2
2. User Requirement	3
3. Analysis of Limitations and Drawbacks of existing Altimetry Products	7
3.1. Limitations/Drawbacks in Open Ocean	7
3.1.1. Limitations in Resolution	7
3.1.1.1. Observations of Ocean Phenomena	7
3.1.2. Limitations in Precision and Accuracy	8
3.2. Limitations/Drawbacks in Coastal Areas.....	9
3.2.1. General Limitations in Conventional Coastal Altimetry	9
3.2.2. General Limitations in SAR Coastal Altimetry	10
3.2.3. Limitations in Sampling and Resolution.....	10
3.2.4. Limitations in Accuracy and Precision	11
3.2.5. Other Limitations and Drawbacks.....	11
3.3. Limitations/Drawbacks in Polar Ocean	12
3.3.1. Limitation in sampling and resolution	12
3.3.2. Limitations in Precision and Accuracy	13
4. Review Existing CryoSat-2 L1B SAR products over Ocean	14
5. The Sentinel-3 SAR Radar Altimeter data products.....	15
6. Adaptation of current Ocean processing.....	16
6.1. Processing	16
6.1.1. Numerical SAR waveform models	16
6.1.1.1. Simulation tool.....	16
6.1.1.2. The numerical retracking algorithm.....	17
6.1.1.3. The Look-Up correction Table.....	18
6.1.2. Oversampling.....	18
6.1.2.1. Interests for Polar Ocean and Coastal.....	18
6.1.2.2. Current CryoSat-2 product over Open Ocean	19
6.1.3. Along-Track Hamming weighting function	19
6.1.3.1. Interests for removing ice returns	19
6.1.3.2. Drawbacks over Open Ocean	20
6.1.4. The antenna pointing issue	21
6.1.4.1. Ocean retracker with injected mispointing information	22
6.1.4.1.1. Computation based on the use of the RDSAR estimated mispointing	23
6.1.4.1.2. Measuring the pitch angle of the antenna using the SAR mode data	23



- 6.1.4.2. 5-parameters retracker..... 24
- 6.1.5. Data editing 24
 - 6.1.5.1. Waveforms Classification..... 24
- 6.2. Geophysical corrections 26**
 - 6.2.1. Computing the sea level anomalies..... 26
 - 6.2.2. Wet troposphere 26
 - 6.2.3. Dry troposphere 29
 - 6.2.1. Ionospheric correction 30
 - 6.2.2. Dynamical atmospheric correction 30
 - 6.2.3. Ocean tide 30
 - 6.2.4. Solid Earth tide 31
 - 6.2.5. Pole tide..... 31
 - 6.2.6. Mean Sea Surface..... 31
 - 6.2.7. Sea Sate Bias 31
- 6.3. SAR mode coverage and in-flight validation 32**
- 7. References 33**



1. Introduction

1.1. Aim

This document presents a framework of guidelines intended to support the current Copernicus development activities in developing new, technically innovative products and applications over ocean in order to keep up with quickly evolving user expectations and needs.

The Sentinel-3 mission of ESA and the EC is a new element of the Copernicus program that will carry a SAR radar altimeter promising science benefits and enabling to respond to a set of Copernicus user requirements. The Sentinel-3 mission with its SRAL instrumentation contains new features and capabilities as compared to the conventional radar altimeter mission. These form the basis for new innovative Copernicus products and applications that are not considered or implemented in the Copernicus services yet. To utilize the full potential of SRAL data and optimize the retrieval of the geophysical parameters, new algorithms and enhanced corrections need to be developed and also fully tested using CryoSat-2 SAR mode data to ensure that any unforeseen but undesirable impacts of SAR altimetry are fully characterized prior to the launch of Sentinel-3.

Initial CryoSat-2 SAR mode ocean performances, metrics and algorithms have already shown significant progress, offering exciting new perspectives for oceanography, and providing significant experiences to maximize the possible achievements of the Sentinel-3 topography mission. Nevertheless, many scientists expressed the need to further consolidate these results, by collecting more CryoSat-2 data and undertaking further evolutions and improvements in our scientific understanding and technical capability for processing SAR mode altimeter data. Equally important, the geophysical parameters resulting from the upgraded service chains must within reasonable limits be designed to enable delivery the LOTUS WP5 applications of new Copernicus data in value-adding ocean services.

This document specifies the scientific requirements that have been drawn from the experience gained to date through the use of recently analyzed CryoSat-2 SAR mode data together with conventional altimeter data and others research activities and findings relevant to SAR altimetry. It will also outline the applicability and gaps of the derived geophysical parameters for the LOTUS value adding ocean services. This task will use primarily as inputs the results of analyses performed in the framework of past or on progress projects and include a new set of LOTUS value adding ocean services technical requirements.

Based on these scientific requirements, the report provides a critical analysis of current used techniques and methods for each of the three ocean focus areas: open ocean, polar ocean and coastal zone. It also suggests potential alternatives or enhancements for further research directions that would provide substantial improvements of the SAR retrieved sea surface heights, wave heights and wind speeds over ocean, and may drive recommendations for the preparation of the take-up of the Copernicus Sentinel-3 Surface Topography Mission SRAL L2 data. Nevertheless no provision has been included in this document for new processing algorithm studies.

This document represents the deliverable D1.2 of LOTUS - an EU FP7 project that supports the development of Copernicus by developing applications of Sentinel-3 to complete the space observation infrastructures that are designed for land and ocean monitoring for Copernicus.

A list of reference and sources, many of which are available online, is included at the end of the document.



1.2. Document content

This document is arranged as follows:

- Section 2 reviews the user scientific expectations for enhanced Sentinel-3 altimeter SAR applications over ocean as well as the scientific requirements of the LOTUS value adding ocean services technical requirements. This review is based on scientific results available in the public domain in the form of published papers, open-access reports and presentations at conferences as well as analysis of the project specific additional requirements.
- Section 3 is a discussion of limitations and drawbacks of existing altimetry products for the three different ocean areas.
- Section 4 presents the current CryoSat-2 SAR products over ocean.
- Section 5 presents the established Sentinel-3 data products.
- Section 6 defines a list of adapted methods and enhancements that fit for the scientific exploitation of the future Sentinel-3 products in each of the three oceans sub-themes and the LOTUS value adding ocean services.
- Section 0 provides a list of references to the papers and sources used in this document.



2. User Requirement

This section presents a list of scientific and operational requirements based on the results from the CP40 (Cryosat Plus for Ocean) user consultation survey ([Clarizia et al., 2012]), as well as on reports and documentation available from other projects: PISTACH project [Dufau et al., 2008, 20011], Coastalt project [Cotton et al., 2008], SAMOSA project [Moreno et al, 2008]. Finally, an analysis of the technical requirements of LOTUS value adding ocean services is provided.

The main objectives of CP40 were:

- to build a sound scientific basis for new scientific and operational applications of Cryosat-2 data over four different areas, which are: open ocean, polar ocean, coastal seas and sea-floor mapping.
- to generate and evaluate new methods and products that will enable the full exploitation of the capabilities of the Cryosat-2 SIRAL altimeter, and extend their application beyond the initial mission objectives.
- to ensure that the scientific return of the Cryosat-2 mission is maximised.

Since LOTUS is addressing the same areas (open ocean, polar ocean, coastal seas) and exploiting the same kind of altimeter data (PLRM and SAR) as CP40, it seems natural to re-use the CP40 user requirement document as part of the LOTUS user requirements. The document gives the results of a user consultation carried out by the CP40 team, followed by an analysis of limitations and drawbacks of existing products, to finally come up with a list of scientific and operational requirements, per sub-theme. In this chapter, we don't want to reproduce all the results given in this document but only to give the main outcomes of it.

The questionnaire was distributed by email to a large number of users. Some of these users had already been contacted for the COASTALT and PISTACH projects, while some others were new and identified within CP40. In addition to emails, the questionnaire was distributed to participants of the 6th Coastal Altimetry Workshop in Riva del Garda¹, Italy, from 20th to 21th September 2012, and to the 20 Years of Progress in Radar Altimetry (20YPRA) Symposium and the Ocean Surface Topography Science Team (OSTST'12) meeting, both in Venice, Italy, from 24th to 28th September 2012. Part of the WP1000 team for CP40 (Starlab and SatOC) participated to these conferences through a poster [Clarizia et al., 2012] on the initial results from WP1000.

The CP40 questionnaire was designed by the WP1000 team (Starlab, NOC, DTU and SatOC) on the basis of the COASTALT and PISTACH questionnaire, with some modifications and with added questions.

The questionnaire is divided in various sections each with a different objective. The initial sections establish the **user profile**, a **user area of expertise and applications**, with respect to the four sub-themes under analysis, and the **physical processes** that constitute his/her main interest. The subsequent sections focus on the **product characterization** in terms of spatial/temporal sampling and data delivery time requirements, data provision and resolution, and **accuracy** and **precision** requirements. A simple explanation of the concepts of *accuracy* and *precision* was provided at the end of the questionnaire.

Finally, the user is questioned about his/her requirements in terms of **auxiliary data** (including other remote sensing data and a mean dynamic topography) and on the preferred **data format and distribution**.

The information provided through the user survey can be used in combination with existing literature to draw the limitations and drawbacks of existing altimetry products, as well as the user requirements for new altimetry products. A total of 21 users responded to the CP40 questionnaire, and their response has been merged with those from the past COASTALT survey, for a total of 41 replies. In some cases, the answers has also been merged to those from the PISTACH survey, achieving a total of 71 replies.

¹ <http://www.coastalt.eu/gardaworkshop12>



It has to be taken into account that the majority of the users who responded to the COASTALT and CP40 surveys come from public sector (80%) and the research field, and the majority of users are experts in coastal areas (63%) and open ocean (31%). There is a lack of participation from the private sector (20%) and from the polar ocean and sea-floor mapping community (only 3% each). Hence, the questionnaire is complimentary to the more commercially driven downstream service user requirements presented subsequently.

Generally speaking, the main points of the questionnaire can be summarized as follows:

- I. The majority of the users have already used altimetry data for their work or research.
- II. Most users study the ocean through remote sensing data, followed by numerical modelling and in-situ measurements;
- III. The majority of users still consider their work to be in delayed mode. However, a non-negligible percentage of them works with Real Time (RT) or Near Real Time (NRT) data;
- IV. Datasets longer than one year are the preferred ones by the majority of the users;
- V. The predominant area of expertise of the users interviewed is the coastal area (including both near-shore and coastal zone), followed by open ocean.
- VI. The altimetric products are mostly used for model validation, and as a diagnostic for oceanic processes.
- VII. For open ocean, the majority of users need altimetry data in several regions around the globe;
- VIII. For coastal zone, the majority of users are interested in the coastal strip between 0 km and 50 km, and they are also interested in several coastal locations.
- IX. The two major physical processes of interest are Sea Level Anomaly (SLA) and Sea Surface Height (SSH); Surface Elevation is considered the most important parameter.
- X. The along-track posting rate mostly used is 1Hz, but a clear preference emerges for 20 Hz. Some users express the wish to have FBR data available.
- XI. The users express a need for a better along-track resolution for the future.
- XII. Most users still use and prefer offline data, but there is a clear shift of the demand towards data with shorter latency (NRT and RT).
- XIII. Users want the products to have the best possible accuracy and precision for height and SWH;
- XIV. Even though only a few users responded to this question, there is also a need for a better precision and accuracy in σ_0 (radiometric) measurements;
- XV. Users call for products that include quality control information, auxiliary data for instrument and geophysical corrections (atmospheric, tides, etc.) and auxiliary reference data (e.g. MDT, geoid);
- XVI. Optical and SAR data are the most used ones as synergistic remote sensing data;
- XVII. The most used and preferred data format and delivery remain NetCDF and *ftp* respectively;
- XVIII. The majority of users both use and prefer altimetry datasets to be updated on a daily basis.

As a general consideration, the results after merging the CP40 survey contributions confirm the previous user needs from the COASTALT and PISTACH survey. Only a few aspects have changed (i.e. there are now more users using remote sensing than those using numerical modelling), while some important needs, already emerging from the COASTALT and PISTACH surveys, have been strengthened by the CP40 survey (i.e. need for better resolution, need for better precision and accuracy).

We must however notice that these requirements have been mainly done for level 2 products. In our case, LOTUS is aiming at providing also higher level products (L3 and L4). Level 3 are multi-missions products while Level 4 are gridded products.

LOTUS also aims at exemplifying user driven products where the altimetry data enters as a component of a more complex analysis relying on satellite, model as well as in-situ data. In this light, the user requirements collected above relates rather well to the overall requirements of the downstream component of LOTUS viewed as a user.



However, a number of more specific requirements are requested for the LOTUS value adding ocean services. The following paragraphs will describe these per product with relevance for the SRAL data products, i.e. Task 5.1, Task 5.2, Task 5.3 and Task 5.5.

Task 5.1 Improved wave and wind design data

Task summary: This task will use the high resolution wind speed and wave height product from the SRAL SAR to improve the description of the high frequency and wavenumber components in deriving wave and wind design data in marine engineering. The new more high frequent spatial correlation scales of significant wave height and wind speed are important in this respect and can be integrated with modelling and in situ data via ergodicity for design data studies and related cost sensitive decision making. Potential application: Offshore Wind farms

Task scientific requirements beyond the updated CP40: This task requires SWH at improved spatial resolution. However, the length scales of e.g. storm waves typically have a wave length of 150-200m and hence sampling of these waves become an issue if a higher spatial sampling is sought. Presently, in situ data provides estimates of significant wave height sampled over 20 min and collected every 30 min. Over the same period the long storm waves can travel 20-30 km and shorter more high frequent waves a shorter distance. Hence, in order to estimate the significant part of the wave spectrum that is not resolved in in situ data the SWH processing of the SRAL data must be explored at sampling intervals ranging from 300 to 1000m in the lower end and up to the existing 1Hz data in the upper end. Issues of signal to noise ratio must also be explored as well as the impact of wave direction (taken from models) on the analysis accuracy. The North Sea will constitute a good test case.



Figure 2.1 Example of wind mill farm in the North Sea that would have benefited from more accurate estimates of high frequent part of the wind sea spectrum

Task 5.2 Characterization of coastal scale hydrodynamics.

Task summary: The availability of accurate water level and wave height observations at 350m resolution is close to the spatial scale of wave groups and hence can be used for the estimation of conditions causing surf beat. Combination with the wind product as well as in situ and model estimates of wind velocity and wave spectra will allow addressing the aliasing of the signal and the wave direction and hence the periods and amplitudes associated with surf beat and potential local seiching in inlets or harbours. To the extent these signals can be proven to depend on particular conditions available in classical metocean data, a risk forecast of the phenomena can be developed. In addition detailed analysis of transient water level response to wind forcing in shallow seas, coastal jets and basin scale seiching is addressed using a combination of SRAL SAR and numerical modelling.



Task scientific requirements beyond the updated CP40: Two main challenges to conventional altimetric products are posed by this LOTUS service. It requires high spatial resolution in line with SRAL and it is of relevance in areas relatively close to land (1-20km). The length scale of the wave groups is of the order kilometres but dependent on the peakedness of the wave spectrum. The method further requires a fair estimate of the direction of wave groups, which comes from in situ data or models. Physically, the product is also challenged in areas where other physical processes have similar spatial scales and comparable amplitude, although modelling can to some extent be used to disentangle the signals. Hence it as a requirement for the SRAL product to provide a true SSH at the highest possible spatial resolution with no smoothing implicitly acting as a spatial low pass filter. Further, the data should be accessible in a common mode from off shore to near the shore. The Northern Adriatic Sea will constitute a good test case.

Task 5.3 New current design and forecast data

Task summary: This task will explore the combination of high resolution altimetry data and modelling of meso- and submesoscale processes on the continental shelf and shelf break. The SRAL SAR data and the availability of the newest GOCE based geoids allows a new level of accuracy of absolute sea surface height to be provided in very high along track resolution with an error description. At the same time, new generations of ocean models such as ROMS or MIKE 3 FM model nearly all water level causing phenomena in increasing resolution now resolving the mesoscale and the submesoscale for selected areas. Hence, the road is paved for introducing a new data assimilation approach in which level 2 data is directly assimilated without correction for tides and barometer effects. This task will demonstrate such an approach while simultaneously integrating the assimilation of AATSR as a complimentary data set. The increased resolution will in particular help the representation of extreme current speeds.

Task scientific requirements beyond the updated CP40: This particular application will make use of the meso- and sub-mesoscale observations available with SRAL due to the increased spatial resolution. Hence one main technical requirement is the 350m resolution. Further, a consistent integration with geoid models and the uncertainty (absolute and spatial correlations) of both the geoid and the SRAL data is optimal. Finally, it is foreseen that this application will necessitate various levels of processing of the along track data with various geophysical corrections included or not (mainly tides, inverse barometer effects and absolute versus relative sea level products). The application is both hindcast, nowcast and forecasts of current velocity and is envisioned for North Sea and/or Gulf of Mexico offshore design data and oil spill protection.

Task 5.5 Climate change services

Task summary: Based on the products for surface currents, eddy detection and front detection developed in WP3 data will be analysed in combination with the current estimates of Task 5.3 and additionally be integrated in the climate change data as assembled in parallel Copernicus climate change projects.

Task scientific requirements beyond the updated CP40:

TBD



3. Analysis of Limitations and Drawbacks of existing Altimetry Products

This section presents an analysis of limitations and drawbacks of existing altimetry products, based on the results from the CP40 user consultation survey as well as on reports and documentation available from other projects ([Cotton et al., 2004], [Moreno et al, 2008], [Cotton et al., 2008], [Dufau et al., 2008a, 2008b], [Cotton, 2010]) and important outcomes from recent altimetry workshops and meetings. This analysis constitutes the main input for the definition of a list of scientific and operational requirements for the new methods, products and applications developed in the context of CP40, and presented in section 0. Even though some of the limitations and drawbacks of current products will be shared across different sub-themes, they are separately identified and analysed for the four sub-themes under analysis in CP40, and they are presented in four separate paragraphs.

3.1. Limitations/Drawbacks in Open Ocean

3.1.1. Limitations in Resolution

A key point that emerges from the user consultation survey is the need for an improved spatial resolution. The resolution of conventional altimetry represents an important limitation for accessing small spatial scales. Conversely, SAR altimetry on board Cryosat-2 represents an unprecedented improvement that should allow reaching the smallest spatial scales, at least in the along-track direction.

Low Resolution Mode (LRM) altimeters provide measurements which refer to a large waveform footprint. The size of the footprint is different for each altimeter and depends on many parameters such as the orbit height, the bandwidth and the number of gates considered in the waveform retracking. Generally speaking it can vary between about 6 and 11 km.

The size of the altimetry footprint determines the resolution of the altimetry itself, and ultimately the capability to adequately observe ocean phenomena, assimilate altimetry data into models, and validate the altimetry products themselves.

Theoretically, 1 Hz LRM data are limited to 14 km resolution (twice the 7 km sampling), while 20 Hz LRM data are only limited by the footprint size. For this reason, the 20 Hz data help to extend the data coverage near the coasts, and allow a better detection of outliers in open ocean (mainly sigma bloom and rain cells).

Nevertheless, the reachable scales are not very small in existing LRM data sets due to the HF noise level. A bump of energy in the Sea Level Anomaly (SLA) spectrum between 10 and 60 km scales can also be observed [Boy et al., 2012] [Thibaut et al., 2013]. Some correlated errors dominate the signal at these wavelengths over most of the open ocean regions. As a consequence, some studies even claim that LRM altimetry is not trustable below 80 km [Xu and Fu, 2011]. This limitation affects both the 1 Hz data and the 20 Hz data of conventional altimeters. The main reasons explaining this bump of energy are provided in [Thibaut et al., 2013].

In the following sub-paragraphs, the limitations in resolution of existing altimetry products are separately identified for three different applications: observations of ocean phenomena, model assimilation and comparison with in-situ data.

3.1.1.1. Observations of Ocean Phenomena

Generally speaking, **limitations in the achievable spatial resolution can translate into limited capabilities to observe some phenomena occurring in the open ocean, particularly those at smaller scale.** As already said, all ocean structures with a spatial scale smaller than 14 km, cannot be resolved with standard altimetry. Short spatial-scale open ocean phenomena like some small eddies and fronts, coastal upwelling, and some of the mesoscale and shorter-scale physical-biological variations cannot be detected. In addition to this, internal waves and tides, important for



ocean mixing, as well as natural and man-made slicks, rain cells, or small-scale wind bursts and convective cells in an unstable atmospheric boundary layer, would all cause rapid variations of the altimetric backscattered coefficient (σ_0) [Cotton et al., 2008]. Intuitively, these variations cannot be detected when the footprint is too large, as for conventional altimetry.

Some big uncertainties also lay in gaining accurate knowledge of ocean currents. Currents derived from altimetry often seem lower than those directly observed offshore, and a non-sufficient spatial resolution seems to contribute to such underestimation [Cotton et al., 2004].

From these considerations, it clearly emerges that the improved along-track resolution from SAR mode data can largely contribute to a new or improved way to observe such phenomena, at least in the along-track direction.

3.1.2. Limitations in Precision and Accuracy

A second important aspect for open ocean issues that has emerged from the survey is the need for a better precision and accuracy, for sea surface height, SWH and radiometric measurements.

An improved precision (lower noise) in the altimetry measurements can lead to improved observations of open ocean phenomena like eddies and fronts, coastal upwelling, and mesoscale and short-scale physical biological-interactions. Phenomena that would benefit from an improved accuracy are instead global warming and sea-level rise and seasonal cycles. El Niño, Rossby waves, internal and surface tides and barotropic variability need both a high precision and high accuracy to be properly observed.

As far as precision is concerned, it has been shown that a reduction of the noise plateau of 30% can be achieved through SAR processing of Cryosat-2 data, compared to the noise level of Jason-2 spectral data [Boy et al., 2012].

In terms of SWH and wind speed, these are parameters that require a high spatio-temporal sampling, as well as a high accuracy and precision of the observations, for the purpose of offshore and shipping operations, operational oceanography and prediction of dangerous sea states, extreme events and rogue wave formation, as well as into wave model assimilation and validation. It has also been demonstrated that a higher precision in the estimation of both wind speed and SWH measurements would allow better estimation of air-sea fluxes (in particular the estimation of global mean air-sea gas transfer velocities), whose climatologies are centrally important in climate studies [Cotton et al., 2004].

Radiometric measurements from altimetry, related to wind speed, have always been particularly difficult, due to the difficulty in calibrating the measurement of backscattered coefficient. Even though it has been claimed that an improvement in the wind speed measurement of about 20% can be reached with SAR altimetry, this calibration issue will have to be tackled and overcome for Cryosat-2, as for conventional altimeters, to be able to obtain better measurements of wind speed and also of Sea State Bias (SSB).

Cryosat-2 SAR data can therefore provide measurements of range and SWH with a two-fold improvement in precision, compared to standard altimeters [Jensen and Raney, 1998, Phalippou and Enjolras, 2007].

The accuracy shown by Cryosat-2 is also quite compelling, especially given that it does not carry a radiometer onboard. However, there are current limitations intrinsically linked to the SAR altimeters, in particular the lack of sensitivity to low SWH highlighted in [Smith, 2012], the current lack of a Sea State Bias (SSB) correction, and several problems and limitations specifically linked to the SIRAL altimeter onboard Cryosat-2 (non-optimal design of pulse transmission mode for ocean, oversampling and hamming window applied to Cryosat-2 data for sea-ice monitoring purposes, which is not optimal for ocean observation). These problems will have to be soon addressed to improve the performance of the SIRAL altimetry onboard Cryosat-2 and of the forthcoming SAR altimeters.

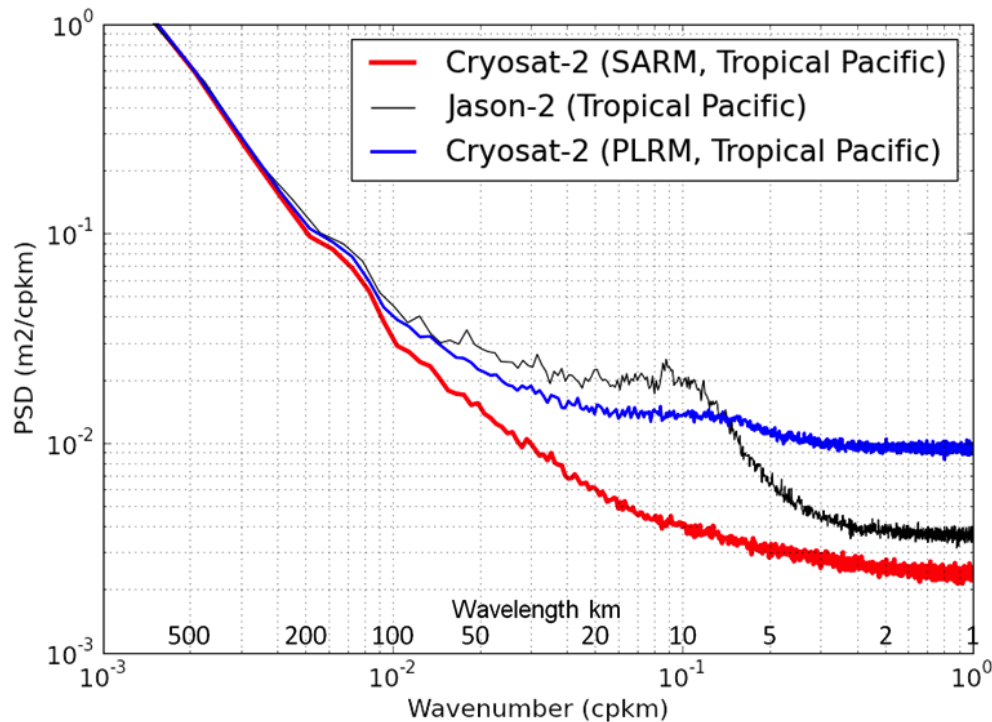


Figure 3.1 : SLA spectra for Jason 2 data (black), Pseudo-LRM waveforms from Cryosat-2 data (blue), and SAR waveforms from Cryosat-2 data (red). The spectral bump is clearly visible and it is located at spectral wavenumbers between 10 km and 80 km. The spectral bump is totally removed with SAR processing [Thibaut et al., 2013].

3.2. Limitations/Drawbacks in Coastal Areas

The outcome of the user consultation highlights that the majority of respondents state their area of expertise to be in the near-shore and coastal zone. This includes both operational and research users. Although the coastal community may be over-represented because of the inclusion of previous results from COASTALT and PISTACH, it nevertheless confirms the strong demand for altimetry products in the coastal zone.

3.2.1. General Limitations in Conventional Coastal Altimetry

Radiometer corrections and the retracking techniques represent the most important current limitations of conventional coastal altimetry.

Radiometer corrections are very difficult from 50 km up to the coast, mostly due to water vapour contamination (which makes the wet tropospheric correction particularly critical in coastal areas). Some important progress has been made in this field within the COASTALT project (www.COASTALT.eu), where an innovative correction (GPD) has been developed by measuring the water vapour delay through GPS signals [Fernandez et al., 2010]. However, this technique still relies on the presence of a number of GPS stations, as well as on integration of measurements with



numerical models. It is therefore clear that progress in the improvements of such correction needs to be sustained.

As far as retracking is concerned, this usually affects a smaller coastal strip (approximately from 10 km away from the coast corresponding to the size of the waveform footprint), but it is an even more complicated issue. Conventional Brown model waveforms are very rare close to the coast, due to the land contamination in the footprint of the altimeter. Furthermore, the impact on the waveform strongly depends on the type of contamination (i.e. bay, sheltered area, land, or even from rain cells or ocean surfaces with inhomogeneous backscattering properties), and the effect on the waveform can be so far fully modeled only in some specific cases.

At present, there is not yet an universal approach for retracking close to the coast, which would work in all coastal conditions. A number of specialized retrackers have been developed within the COASTALT and PISTACH projects, but some of them work for specific types of contamination. In addition to this, discrepancies and biases have been observed between different retrackers [Thibaut et al., 2012]. Beside the difficulty in comparing the results from different coastal retrackers, **this also poses a threat on the continuity of results between open ocean and coastal areas.**

It is clear that, despite such limitations, some important results have been achieved in the last years through COASTALT and PISTACH, and **the effort to recover the information from conventional altimeters close to the coast should be supported in the future, given the current availability of several years of altimetry data in the coastal zone still largely unexploited.**

3.2.2. General Limitations in SAR Coastal Altimetry

SAR altimetry can clearly bring numerous advantages, in that the higher along-track resolution and smaller footprint will imply a weaker land contamination, and the capability to get closer to coastal areas. However, it is worth to point out that this still depends on the orientation of the SAR altimetry footprint with respect to the coast (which is believed to affect the retrieval of SWH in particular [Thibaut et al., 2012], [Thibaut et al., 2103b]), and the morphology of the coast itself.

In terms of retracking, and as for the open ocean, a continuity and consistency of results needs to be achieved with both SAR and pseudo-LRM retrackers, with respect to conventional altimetry retrackers near the coast.

As far as radiometric corrections are concerned, Cryosat-2 does not carry a radiometer onboard, and does not perform dual-frequency measurements to implement the ionospheric correction. Even though the performance of the SIRAL altimeter seems to be quite good even without such corrections, **it is important to assess in the near future the impact of radiometric corrections in SAR altimetry, to what extent they are needed, and which of them is more important, particularly for coastal areas.**

Furthermore, several aspects like the effect of swell direction (given the footprint, which is no longer elliptically symmetric) and mispointing on SAR waveforms are not yet well understood, and need a proper investigation and characterization.

For these considerations, it emerges that **dedicated studies on the exploitation of SAR altimetry data specifically for the coastal zone should be addressed in the near future, in parallel with continuity of support for coastal altimetry from conventional altimetry datasets.**

3.2.3. Limitations in Sampling and Resolution

The user survey has highlighted a need for along-track measurements from (at least) 50km from land, right up to the coast, with high spatial resolution and high frequency posting rate (i.e. 20Hz). For conventional altimetry, 20 Hz data provide a better resolution and therefore better availability near land, but they are also much noisier.



These demands are well met by the capabilities of Cryosat-2 SAR mode in coastal regions, where the higher along-track resolution is combined with a larger number of incoherently accumulated looks to reduce the speckle noise and therefore improve the precision of the measurements. The increased capabilities of Cryosat-2 data to observe small-scale ocean structures near the coast have been recently highlighted with respect to conventional altimetry products [Birol, 2012].

Sampling in general still remains one of the major limitations of the products, both from conventional altimeters and for Cryosat-2 data. The combined spatial/temporal sampling of a single mission is still not favourable for many coastal applications (sustained monitoring of coastal dynamics). As a result of this, altimetry at the coast still needs to be used in combination with in situ measurements and models, but it is currently believed that a full solution to this problem will only come from a constellation of altimeters [Cotton, 2010].

An interest for long (>1 year and for many users “as long as possible”) datasets clearly emerges from the survey. This implies a reprocessing of both all Cryosat-2 SAR data in the coastal zone since science products have become available (July 2010), and also the extraction and exploitation of all available coastal information from coastal datasets from conventional altimetry missions. Current operational Cryosat-2 L2 SAR and LRM products are unable to meet this demand at present. Retracked Cryosat-2 LRM ocean data are available from RADS, but only at 1Hz. WP4000 of the CP40 project will develop the means to retrack Cryosat-2 SAR data with the SAM3 model, but only limited processing in a few case study regions will be undertaken within the scope of CP40.

3.2.4. Limitations in Accuracy and Precision

The demand for high precision measurements of height (< 3cm) can be met by Cryosat-2 SAR mode data processed with the SAMOSA 3 model [Gommenginger et al., 2012]. However, Cryosat-2 SAR mode is unlikely to meet the (strict) demand for height accuracy (bias) less than 3 cm. This is in view of the lack of correction for sea state bias in SAR mode, particularly in the coastal zone (but also for open ocean).

While not many users replied to the questions related to Sigma0 wind speed, it is expected that these parameters will be incredibly useful for SAR mode in the coastal zone, and in some cases essential to address the problem of SSB in the coastal areas. Indeed, the higher spatial resolution, and the short-scale changes of wave field in the coastal environment, are likely to have an impact on corrections like SSB. It is also worth recalling that sigma0 (from which the SSB is derived) remains the most difficult parameters to measure from altimetry, mainly due to the difficulty in calibrating the altimetry returns.

3.2.5. Other Limitations and Drawbacks

The demand for instrument and geophysical corrections to be included in the Cryosat-2 SAR products is only partially met by operational products at present. Further work is needed to determine to what extent the information in existing Cryosat-2 L1B and L2 products addresses the needs of ocean and coastal users.

The request for Mean Dynamic Topography in Cryosat-2 SAR products in the coastal zone will also need to be given further consideration. The spatial resolution and accuracy in the coastal zone of existing MDT products is inadequate at present for coastal applications and it is questionable whether MDT would be of any value to altimetry users in the coastal zone.



3.3. Limitations/Drawbacks in Polar Ocean

The main conclusions from the survey with respect to Polar Ocean largely follow the conclusions for the Open Ocean as the Polar Ocean is basically an Open Ocean with the complication of the presence of sea ice.

3.3.1. Limitation in sampling and resolution

Conventional Altimetry naturally suffers from a polar gap, which means that the orbit of conventional altimeters is such that only data within a certain latitude has always been available. Such limitation has been overcome with Cryosat-2, which is a satellite primarily dedicated to monitor sea-ice and polar regions. With its 369 days repeat orbit, at an inclination of about 92 degrees and an altitude of 717 km, Cryosat-2 covers almost all polar regions. Furthermore, the orbit configuration is chosen for optimum mapping of the cryosphere and ice-sheets, where the interferometric capabilities of the instrument provides uniform along-track and across-track coverage with this configuration.

As opposed to the Open Ocean, the Polar Ocean is located at such high latitude that the across-track distance (8 km at the Equator for a 369 days repeat) will become less than 3 km at 70° latitude, which is the southernmost limitation of the Arctic Ocean. With an across-track distance of 8 km on average, the tracks are very close to each other, and will have more than 60% identical footprint. Consequently, this type of orbit can be considered to be a near-repeat orbit. Moreover, some of the Polar Ocean oceanographic phenomena (approximately those with an extension > 10 km) are sampled with an equivalent repeat period that is much shorter than the nominal 369 day repeat period of CryoSat-2.

The temporal sampling of CryoSat-2 altimetry is therefore even improved in the Polar Regions, where the track distance narrows as mentioned previously. Parameters like SWH and wind speed, which require a high spatio-temporal sampling, can in this sense be in principle better sampled in the Polar Ocean than in general in the Open Ocean. However, a thorough investigation should be made to establish the accuracy of this statement. The limitation in resolution presented for Open Ocean, and linked to the footprint of LRM altimeters, is also largely reduced in the Polar Region as SAR mode is used in Cryosat-2 throughout most of the Polar Regions. However, in a very small and limited part of the North Atlantic the LRM is still applied up to 78N, and this still constitutes an important drawback. Nevertheless, the Cryosat-2 mask is not constant in time, and the LRM mode for such region is only applied during the summer month. In some coastal region and some test regions the SARIn mode is also applied.

Another important limitation is linked to the Cryosat-2 mode mask, which is not kept constant in time in the perimeter of the Polar Ocean. As a result of this, large and still unresolved jumps of magnitudes up to meters between the LRM and SAR model data are seen in the ESA GDR products [Andersen, 2012].

While some ocean phenomena (particularly the small-scale phenomena) could not be detected so far with conventional altimetry in polar oceans (i.e. Envisat, ERS-2 and ERS-1), these can be now in principle better seen using SAR altimetry, at least in the along-track direction. Generally speaking, improved along-track resolution from SAR mode data can largely contribute to a new or improved way to observe small-scale phenomena in polar oceans, provided that the accuracy of the measurements is sufficiently high.

It is very important that with the SAR mode the comparison between in-situ observations and altimetry will become “more comparable”, and particularly for the Polar Regions where the SAR mode is applied throughout. Validation is of utmost importance to maintain altimetric accuracy. While most of the in-situ data used to validate these measurements (i.e. tide gauges, oceanographic buoys), are essentially relative to a single point in space with the SAR mode applied the comparison is naturally over a region, but a far smaller region than for LRM data.



3.3.2. Limitations in Precision and Accuracy

Generally speaking, the considerations on limitations in precision related to conventional altimeters, and the precision improvements brought about by Cryosat-2 SAR mode data, illustrated for open ocean in section 3.1.2, apply also for Polar oceans.

However, there are some differences between the two types of ocean in terms of accuracy. **Measurements in Polar regions are frequently characterized by lower accuracy, due to the presence of sea ice which contaminates the radar reflections. This might result in periodic out-takes of data, as well as less accurate data compared with the open ocean.** Even the accuracy of the CryoSat-2 in the Arctic Ocean is far from the standard of existing satellite observations from Envisat / ERS-1 / ERS-2, as CryoSat-2 is not considered operational and as processing is constantly updated in the ESA records which clearly limit the accuracy over [Andersen, 2012].



4. Review Existing CryoSat-2 L1B SAR products over Ocean

LOTUS is necessarily relying on Cryosat-2 SAR mode data for preparation of test datasets over ocean, inland waters and land that can be used in place of Sentinel-3 data prior to launch. These will be used to develop and test new value-added applications for the Copernicus ocean and land services.

At present, no CryoSat-2 Level-2 data products based on this SAR mode data are provided or used operationally. Furthermore, Cryosat-2 L1B SAR products that are generated by the ESA Instrument processing Facility (IPF) are not presently suitable for scientific exploitation over water surfaces.

Cryosat-2 SAR L1B products are currently available for two versions:

Baseline A	July 2010 - December 2012
Baseline B	February 2012 - onwards

The main difference between Baseline A and Baseline B is the use of finer gate spacing in Baseline B (half that used in Baseline A). Given that the number of gates is unchanged (128), this finer gate spacing results in a truncation of the trailing edge of the waveform.

The change to Baseline B was motivated primarily by the need to improve the performance of Cryosat-2 over sea ice. The transition to Baseline B processing for the Cryosat-2 products available on the data dissemination ftp server became effective for products from February 2012 onwards.

Another reprocessing (Baseline C) is expected in 2014, featuring the finer gate resolution and non-truncated waveforms (hence, 256 gates in SAR mode).

The Cryosat-2 processing chains have been designed primarily for ice sheets measurement and not intended for ocean purposes. A MLE3 (Maximum Likelihood Estimator solving for range, SWH and power) retracking algorithm has been implemented but without Look Up Tables for the correction of the Gaussian approximation of the Point Target Response. Moreover, the Sea State Bias correction is not provided in the products.

There is no specific SAR or RDSAR processing implemented in the ESA ground processing. When such processing will be implemented, the L2 processing using SAMOSA retracker is foreseen.

Considering L1B products, they have been designed for ice sheet purposes as well (see above our remarks on baseline A and baseline B products in particular with oversampling and Hamming weighting)

For ocean purposes, a new processing chain (Cryosat-2 Ocean Product) has been designed and developed and will be operated from January 2014 (TBC). This chain will process the LRM data set and the SAR data set but only considering RDSAR processing. A SAR processing has not yet been defined for the Cryosat-2 data over ocean. For the LRM and the RDSAR processing, a MLE retracking has been implemented solving for 4 parameters (range, SWH, power and square of the mispointing angle). This processing is known as a MLE4 retracking.



5. The Sentinel-3 SAR Radar Altimeter data products

The established Sentinel-3 SAR Radar Altimeter data products are describes Mission Requirements expressed in the Sentinel-3 Mission Requirements Document [MRD, MRTD].

Because the Sentinel-3 mission is the Copernicus space component for monitoring the ocean, processings have been mainly designed for ocean purposes (LRM, SAR and RDSAR).

Regarding the LRM processing, the processing chain is a classical conventional altimeter processing chain using a MLE4 retracking and considering Look Up Table and Sea State Bias corrections

The SAR/RDSAR L1 processing is very similar to the Cryosat-2 one. As for Cryosat-2, the colocalization between SAR and RDSAR measurements is not guaranteed. However, no across-track oversampling, nor along-track Hamming weighting has been implemented. For the L2 retracking algorithm, the SAMOSA retracking will be used for SAR echoes while for RDSAR, a MLE4 algorithm will be used. Some specific additional retrackers have been defined including the ice-1, sea ice and ice_sheet.

Contrarily to Cryosat-2, Sentinel-3 embarks a bi-frequency altimeter. The ionospheric correction will be computed using range estimates in both frequencies.

Contrarily to Cryosat-2 mission, a radiometer is embarked on-board Sentinel-3. It will provide the wet tropospheric correction.



6. Adaptation of current Ocean processing

The Sentinel-3 mission requires numerous adapted algorithms and enhanced corrections that must be function of the specified scientific requirements, or the mission may not utilize the full potential of the SAR data and not maximize the possible achievements of Sentinel-3 topography mission.

Based on an understanding of the scientific requirements that have been developed previously, this section addresses a list of current algorithms defined in the CryoSat-2 processing chain to be adapted for Sentinel-3 in each of the three “Oceans” sub-themes of interest, namely Open ocean, Coastal zone, and Polar ocean. The scientific constraints for the methods and models to this purpose, and, if any, remedial solutions are discussed.

Similar analysis is performed concerning corrections. Those that are relevant for the retrieval of ocean geophysical parameters are considered.

6.1. Processing

6.1.1. Numerical SAR waveform models

6.1.1.1. Simulation tool

Modelling complex SAR waveforms theoretically need many simplifications (in terms of point target response, antenna pattern...) and the emerging analytical models may not be therefore valid (e.g. the analytical SAMOSA model which is the baseline retracker for Sentinel-3 considers such approximations). Simulation does not require that many simplifying assumptions, making it the most practical tool to handle complex model with an adequate descriptions of the reality. It is particularly relevant when making changes in some aspects of the processing or the instrumental configuration (off-nadir mispointing angles) that are difficult to put into equations or may not be theoretically accounted for. Also improvements in the simulator may be continuously implemented in order to better take into account the actual characteristics of the altimeter (e.g., various shapes of PTR and LPF).

By principle, a numerical simulator is used to generate a SAR echo model that mimics the radar altimeter response in SAR mode (taking into account the real elliptical antenna pattern and a real point target response). It is based on a point-by-point radar response simulation on a gridded surface without limitation of resolution (fully adaptive). The satellite altitude and altimeter characteristics can be modified depending of simulated missions (Jason-2, AltiKa, Sentinel-3, CryoSat, Jason-CS...). A theoretical or measured antenna pattern can be used taking into account mispointing angle in both axes. Theoretical or measured Impulse Responses can be used as well. In addition, the surface height can be modified using a Digital Elevation Model and atmospheric attenuation or ground “reflection anomalies” can be introduced for specific investigations. Figure 6.1 illustrates the different steps of a fully amplitude numerical simulator of SAR echoes [Desjonquères et al., 2012]. Major processes of the SAR simulator are in sequence:

- 1- The power return signals from each point of the gridded surface are computed then sorted by Doppler band and accumulated in the appropriate range gates of the waveforms.
- 2- The flat sea surface response is then convolved with the azimuth and range impulse response (AIR and RIR) of the radar. In [Phalippou et al., 2007], both the RIR and the AIR are approximated by cardinal sin functions, while the antenna gain is simulated with a Bessel function associated with a circular aperture.
- 3- Prior averaging, the Doppler bands are corrected in range to compensate the slant range migration, i.e. to place all observations of a scatterer at the same radial distance from the satellite when the satellite moves along its orbit.
- 4- The Doppler beam waveforms (looks) from the same surface are summed (multilooking) to finally form the SAR echo model for a flat sea surface (the sea wave height is applied “on the fly” in the retracking process to provide an exact solution for the SAR waveform).



- 5- To finish, the simulator convolves the previous result with the PDF of the significant wave height that is taken to be Gaussian, although this method would make it equally possible to use a non-Gaussian sea surface PDF to account for non-linear wave effects.

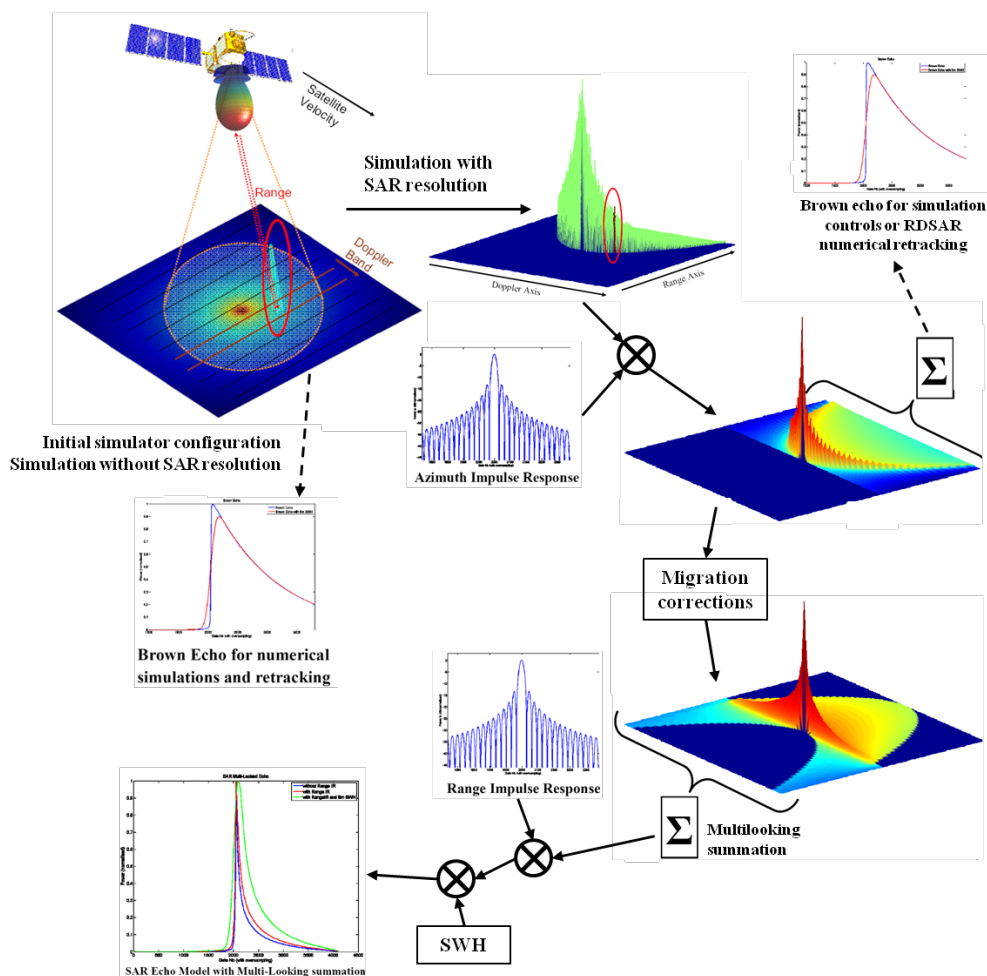


Figure 6.1 : SAR echoes simulator [Desjonquères et al., 2012].

Note that, the simulator can also generate LRM numerical model. In that case, the step 3 is not performed (no range migration). This simulation option is very useful since it is possible to cross compare and validate the simulator with the Brown model.

The validation of the simulation tool consists in generating a LRM numerical model with a real azimuth impulse response but with a Gaussian range impulse response to get the same assumptions than Brown. Then, this model is retracked using a Brown model and the estimated parameters are compared to the simulation parameters. Overall assessment shows very good agreement. Practically differences are less than 1 mm for epoch and 1 cm for SWH.

6.1.1.2. The numerical retracking algorithm

Regarding the L2 SAR-mode processing, a numerical retracking algorithm based on simulation of Doppler echoes model is associated.

The numerical method consists in fitting a Doppler waveform with the pre-computed echo model (generated off-line by a simulator) that is described by known instrumental and geophysical parameters. This method may require huge data storage and, inevitably, long processing times to generate an echo model database with varying sets of sensitive parameter values (sea-state, satellite parameters) and with small sampling intervals. In implementing this strategy, the goal is to



build a database in a way that ensures the accuracy and precision of the estimates. This may highlight some difficulties that should be considered in future or related work.

As for conventional altimetry, the ocean parameters estimated from the numerical SAR retracking are expressed as:

$$\theta_n = \theta_{n-1} - g(BB^T)_{\theta_{n-1}}^{-1} (BD)_{\theta_{n-1}}$$

Where θ_n is the estimated parameter at iteration n ; B, D are the partial derivatives and residuals matrix, and g is the loop gain (between 0 and 1).

For unsolved analytical model, derivatives of the mean return power can be computed numerically. The method consists in approximating the derivatives by a finite difference involving the database of pre-computed echo models. At each iteration n , models using the current estimation vector θ_{n-1} are directly taken from the database. The performances of this method have been evaluated theoretically using simulated LRM waveforms and, have been statistically validated on real data by applying it on Jason-2 raw measurements. The results are found to be consistent with those obtained from a classical MLE4 retracking.

The numerical SAR retracking is based currently on a 3-parameters model that accounts for varying off-nadir mispointing angles provided by the star trackers.

6.1.1.3. The Look-Up correction Table

The triple convolution that defines the echo numerical model (identical to the equations provided by Brown on conventional altimeters) is then computed numerically to provide an exact solution for the SAR waveform, without the need for approximations. This is the method adopted by TAS [Phalippou et al., 2007], [Phalippou et al., 2011] and by CNES [Boy et al., 2012]. In this case, there is no need of using a Look-Up correction Table.

The LUT is used to correct the estimated parameters (range, significant wave height and σ_0) for errors resulting mainly from the Gaussian approximation of the Point Target Response (PTR) in the conventional Brown ocean retracker (others effects are also included in the correction LUT like the quantization of the signal, fast Fourier transform, speckle noise, etc.). Some investigation is currently underway to update this correction LUT taking into account not only the approximation of the PTR in the retracking algorithm but also the characteristics of the radar altimeter (notably the ellipticity of the antenna for CryoSat-2) and the particular speckle reduction property of the RDSAR method (different from conventional altimetry mode).

6.1.2. Oversampling

In some situations where the surface targets are very specular (e.g. sea ice or at very low sea states in coastal zones) or when the satellite rate of change of altitude is particularly large, the squaring step in the SAR power processed data may lead to some aliased power echo waveforms and then to the loss of some of the resolution. The result rendered SAR L1B data highly degraded typically over specular surfaces in polar ocean or coastal.

6.1.2.1. Interests for Polar Ocean and Coastal

To solve that, raw complex SAR echoes are oversampled (broadening the leading edge of the waveform). This method consists, as suggested by Jensen et al. (1999), to extend the frequency domain to 256 bins by padding the 128 existing ones with zeros, and then do the Fast Fourier Transform to obtain 256 complex gates (with twice the resolution) in time domain. However, although the sampling has changed, the resolution has not since it is fixed by the instrument impulse response.



In addition, it is noted that LRM sampling remains the same as sampling is fixed onboard and oversampling of the on board complex data is not possible. The LRM altimetry data are then continuously affected by aliasing in these regions.

6.1.2.2. Current CryoSat-2 product over Open Ocean

In general, the aliasing effect is considered negligible over diffuse surfaces such as ocean.

Since February 2012, raw complex SAR echoes from CryoSat-2 are oversampled in the FBR to level-1b processor (baseline B products) in order to avoid aliasing over strongly specular targets (e.g. sea ice), which are of primary sites of interest for this mission. Given that the number of samples per waveform remains unchanged (i.e. 128 samples), this results in the truncation of the trailing edge of the waveforms that may lead to inaccurate estimation of wave heights, making the method not appropriate for the open ocean studies. Any user of the data needs to take this into account when using waveforms and determining range.

6.1.3. Along-Track Hamming weighting function

6.1.3.1. Interests for removing ice returns

In a normal SAR processing scheme, the azimuthal FFT may consider the application of a weighting function box like in along-track direction, and the corresponding impulse response is a cardinal sin function [sinc or $\sin(x)/x$] as shown in top of the Figure 6.2.

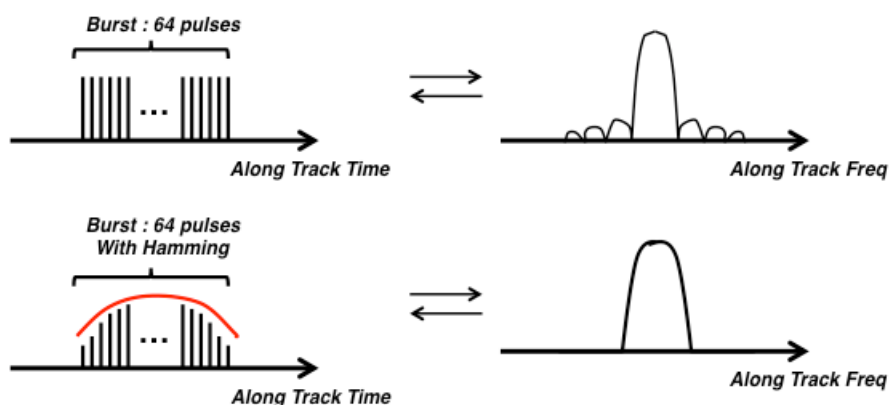


Figure 6.2 : The resulting weighting function without (top) and after (below) the application of Hamming window in along-track direction

Based on this process, it became clear that some high levels of energy contained in the main lobe are spread into side lobes of the azimuthal impulse response, then impacting the SAR L1B waveform shape. This is particularly evident for highly specular reflections over sea ice where the very strong nadir echo leads to spurious signals in the beams pointing off nadir, which is the clutter in this case. This can be seen on the left of the Figure 6.3, showing nadir clutters as parabola features mainly present in the leading edge of the SAR echo waveforms. This result renders SAR L1B data highly degraded over specular surfaces, particularly in Polar ocean but also in coastal zones.

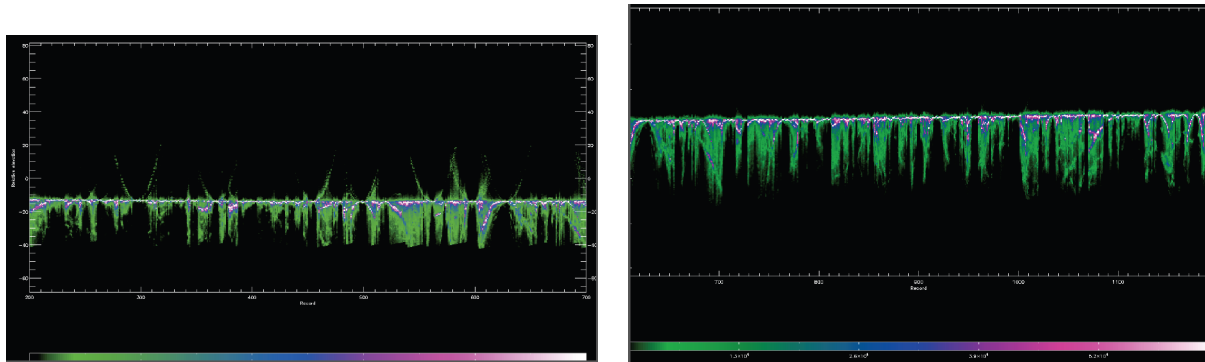


Figure 6.3 : Cryosat-2 SAR waveforms over sea ice before (left) and after (right) along-track Hamming weighting (Courtesy Rob Cullen, ESA)

The CryoSat-2 Baseline B processing is designed with the application of a Hamming window in azimuth direction, to all samples of all echoes of every burst, in order to reduce the side lobes effects (see Figure 6.2). A typical azimuth impulse response of CryoSat-2 SAR burst is characterized with and without hamming window in Figure 6.4 [AD3]. This windowing process eliminates clearly the nadir clutters as shown in the CryoSat-2 SAR echo waveforms of the Figure 6.3 for those that are processed with an along-track Hamming function.

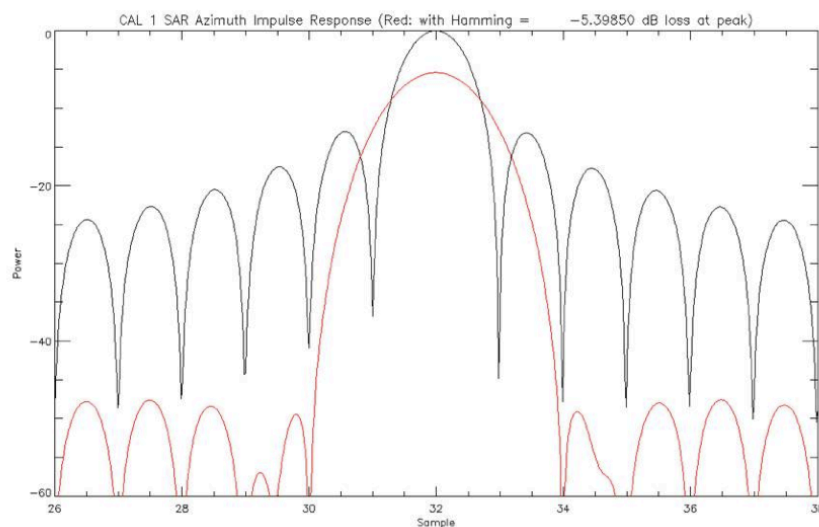


Figure 6.4 : CryoSat-2 AIR with and without Hamming window (zero-padding of 64) [AD3]

6.1.3.2. Drawbacks over Open Ocean

The original along track sampling resolution in SAR mode is then affected by the beam widening effect of the azimuth Hamming weighting function which degrades the resolution. The effective resolution (as opposed to sampling) of the beams is then widened by a factor of approximately 1.3 in the along track direction. This effect, which helps to address aliasing issues over highly specular reflections over sea ice, is nevertheless detrimental to the exploitation of SAR data over water, where some of the benefits of SAR altimetry will be lost. In addition it may modify the pulse-to-pulse correlation properties as what is seen on RA-2 with the cross track PTR.

Thus, for open ocean applications, the Hamming function is not recommended. If CryoSat-2 L1B products are to be used, it seems more appropriate to use data obtained with Baseline A or wait for the release of the data processed with Baseline C.



6.1.4. The antenna pointing issue

It is known that CryoSat-2 is flying nose-up [Galim et al., 2013] with an additional significant roll value. Depending on the behavior of the antenna gain for different values of mispointing, as expected, the across-track mispointing (Figure 6.5) moves the maximum of the antenna gain along the x axis (across track direction) while the along-track mispointing (Error! Reference source not found.) moves the maximum along the y axis (along track direction). This will induce different effects on the corresponding multi-look echo. The along-track mispointing reduces the amplitude of the multi-look echo as shown in Figure 6.6 (left) while it does not change the shape of the normalized waveforms. The across-track mispointing reduces the amplitude of the multi-look echo as shown in Figure 6.5Error! Reference source not found. (right) but it also changes the shape of the normalized waveforms.

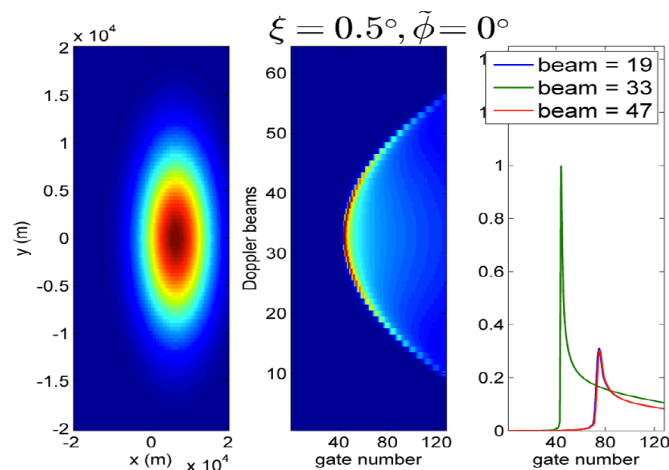


Figure 6.5 : Antenna gain, DDM, and Doppler echoes representation for an across-track mispointing ($\xi_{ac} = 0.5^\circ$ and $\xi_{al} = 0^\circ$) [Halimi, 2013]

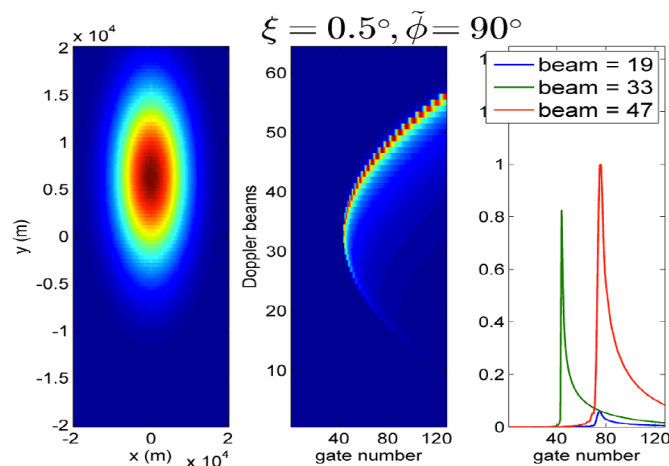


Figure 6.6 : Antenna gain, DDM, and Doppler echoes representation for an along-track mispointing ($\xi_{ac} = 0^\circ$ and $\xi_{al} = 0.5^\circ$) [Halimi, 2013]

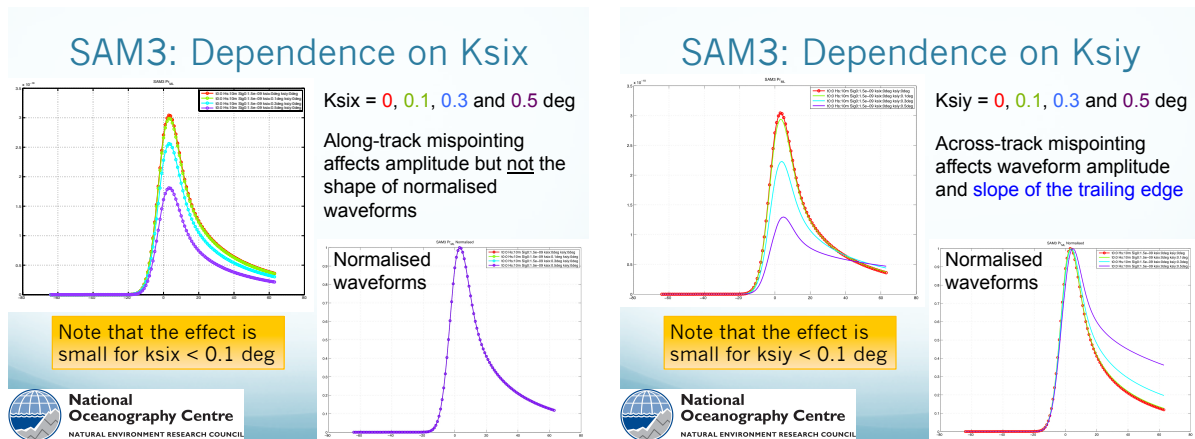


Figure 6.7 : Dependence of the SAMOSA-3 model on (left) along-track and (right) across-track mispointing [Gommenginger et al., 2011].

These analyses have shown that the shape of the delay/Doppler waveform is affected by the value of the across-track mispointing angle ξ_{ac} whereas ξ_{al} has an impact on the waveform amplitude mainly. Note that changing the value of P_u can compensate the change of amplitude due to ξ_{al} . Indeed the along track mispointing angle and P_u exhibit similar effect on the shape of the multi-look SAR waveform as shown in Figure 6.8. This ambiguity can't be resolved by considering the use of a multi-look SAR waveform model retracker (estimating ξ_{al} and P_u) unless it exploits the full DDM (aka 2D waveforms) for which the along track mispointing angle is different in this case from that of P_u Figure 6.7, or uses the star tracker attitude information, if reliable, to derive an along-track mispointing value to be injected in a retracker (of 3-parameters: range, significant wave height, amplitude).

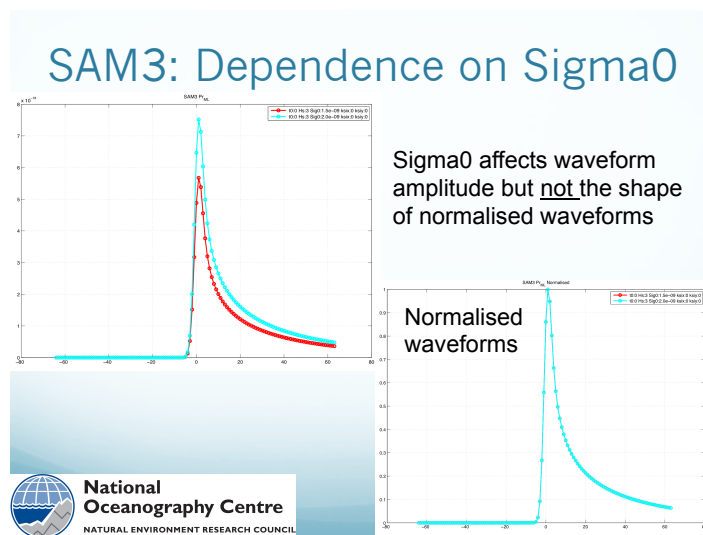


Figure 6.8 : Dependence of the SAMOSA-3 model on Sigma0 [Gommenginger et al., 2011].

6.1.4.1. Ocean retracker with injected mispointing information

The accuracy of the resulting retracked parameters is a function of the ability of the star tracker to give accurate information and the way the angular biases are calculated to align the star tracker information on the altimeter electromagnetic axis.

Different approaches may be considered to measure the off-nadir mispointing angles.



6.1.4.1.1. Computation based on the use of the RDSAR estimated mispointing

The following method consists in estimating the angular biases (a, b) corresponding to the angular alignment between the star tracker boresight and the altimeter electromagnetic axis in both directions (along-track and cross-track directions). This duplet values must satisfy the criterion below, for all data that are contained in a large time period (where biases should be stable):

$$\begin{aligned} \xi_{ac} &= \xi_{roll} + a \\ \xi_{al} &= \xi_{pitch} + b \end{aligned}$$

where ξ_{ac} and ξ_{al} are the off-nadir mispointing angles, and ξ_{pitch} and ξ_{roll} are the star tracker information

To find the roll and pitch biases an iterative least-square estimation method is used that consists of minimizing the errors between the mispointing angles ξ^2 estimated from LRM data and the mispointing angles, $\xi_{ac}^2 + \xi_{al}^2$, obtained from star tracker.

$$\xi^2 - [(\xi_{roll} + a)^2 + (\xi_{pitch} + b)^2] = 0$$

The solution corresponds to the minimum mean squared error estimator as shown in Figure 6.9. Then, the biases are added to the star tracker information to get the mispointing angle of the antenna in both axes (in along-track and cross-track directions) that are injected as input to the SAR (and RDSAR) 3-parameters retracker.

This method is recommended by the NOAA [Smith et al., 2011] and CNES [Boy et al., 2013].

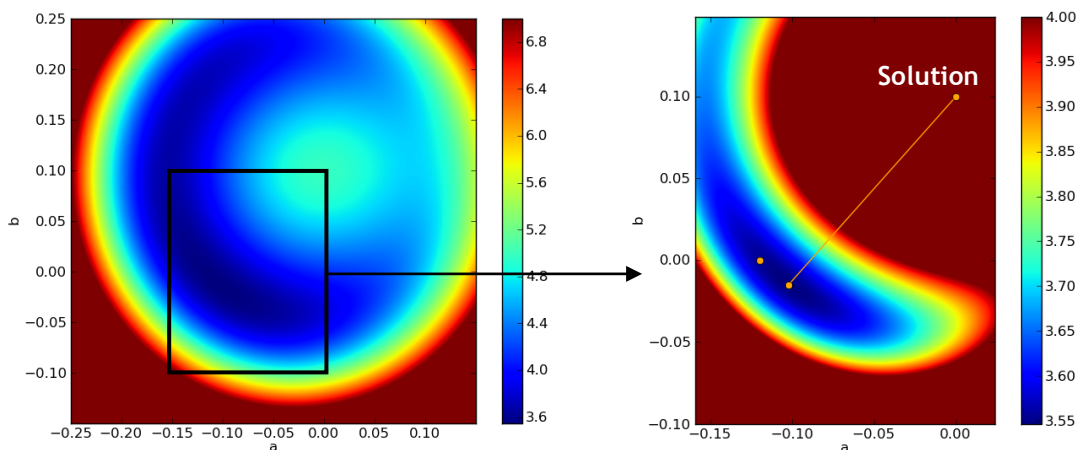


Figure 6.9 : Square errors calculated for different values of a and b [Boy et al., 2013].

6.1.4.1.2. Measuring the pitch angle of the antenna using the SAR mode data

When CryoSat-2 is flying pitched, asymmetrical weighting of echo power in the forward and backward looking beams resulting from the along-track antenna gain pattern can be used to measure its pitch (along-track mispointing angle).

The Figure 6.10 illustrates the difference in illuminating geometry of a satellite (located at point 'O') flying at a zero and a non-zero pitch. If the pitch of the satellite is zero; hence the power distribution between the beams is not detectably modulated by the antenna along-track gain pattern. If the satellite flies pitched, the antenna gain pattern will asymmetrically modulate the power distribution among beams.

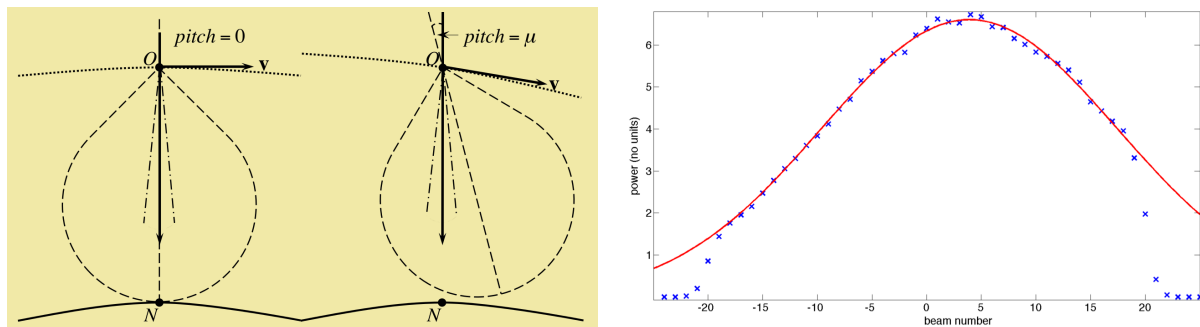


Figure 6.10 : (Right) Figure shows [Galín et al., 2013]

For this last scenario, the Figure 6.10 in right shows an example of distribution of power across the beams that may be found when we average the power in range. The crosses are the mean power within each beam from the data, and solid line is the best-fit Gaussian to the data. The offset between the 0th beam and the maximum of the Gaussian fit is the measurement of pitch [Galín et al., 2013].

6.1.4.2. 5-parameters retracker

The estimation of the 5-parameters vector (including ξ_{al} and P_u) could be achieved when considering the DDM matrix instead of the multi-looked echo. In this case, the along track mispointing angle and the P_u have totally different signatures in the DDM, as shown in Figure 6.8, allowing to distinguish them with the use of a 2D dedicated retracker (to be developed). This strategy may provide better estimation performance as shown in [Phalippou et al., 2012].

6.1.5. Data editing

To analyze the consistency between RDSAR and SAR data in open ocean, only valid ocean data need to be selected. Specific editing criteria are applied:

- a valid flag is used, based on the validation task of CryoSat-2 performed by the CLS Space Oceanography Division. On-board retracked data are used for generating the flag in SAR-mode areas. With noise statistics and the shape of SAR altimeter waveforms so markedly different from those of the on-board LRM, the flag might be not adapted to edit SAR mode data.
- additional editing is applied to make sure to filter out all data points for which the SLA is higher than 1.5m above the reference level. This selection is more severe but ensure to eliminate all outliers (that may be related to some spurious observations caused by rain, blooms, or to some specific events that can occur for instance after an orbit maneuver, or when an anomaly on an instrument impacts the quality of the measurement).

6.1.5.1. Waveforms Classification

Even though the physical processes that induce altimeter signals over deep ocean, coastal areas, polar regions and in inland water, are diverse, the contamination of oceanic waveforms by land or ice returns absolutely damages the data availability and the quality of the geophysical estimations deduced from any altimeter measurements. The variety of waveform shapes that can be obtained depending of the over-flown surface is great and a classification of these waveforms can be useful for the final user in order to determine the confidence he can have on the geophysical parameters that are provided in the products.

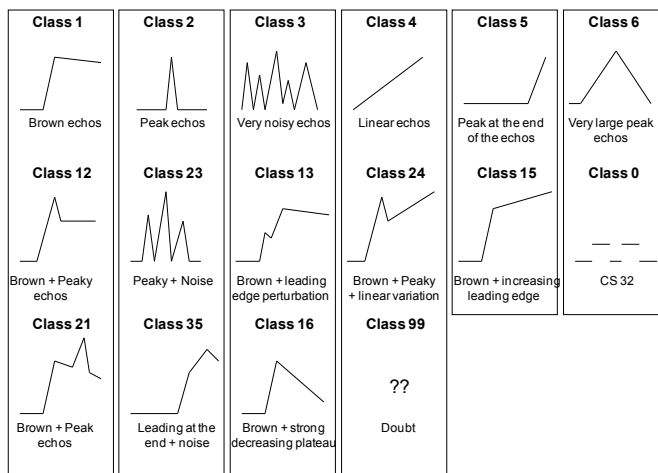


Figure 6.11 : Waveform classification provided in Jason-2 coastal PISTACH products (CNES products) (Thibaut et al, 2010)

Figure 6.11 is an example of LRM waveform classification provided in the CNES PISTACH products. The same kind of classification flag can be provided for delay-doppler altimeter échos.



6.2. Geophysical corrections

6.2.1. Computing the sea level anomalies

Sea Level Anomalies (SLA) are computed by applying geophysical corrections to the uncorrected sea level height. Altimeter standards are the components used in the SLA calculation defined by this formula:

$$SLA = Orbit - Range - \sum_{i=0}^N C_i - MSS$$

where *Orbit* corresponds to the distance between the satellite and the ellipsoid, *Range* is the distance measured by the altimeter between the satellite and the sea surface, *MSS* is the Mean Sea Surface of the ocean over a long period and $\sum_{i=0}^N C_i$ is the sum of all the corrections needed to take into account the atmospheric effects (wet and dry troposphere, ionosphere, inverse barometer) and the geophysical phenomena (ocean tides, high frequency atmospheric effects on ocean) and the sea-surface state (electromagnetic sea-surface bias).

Table 1 shows typical values of the mean and standard deviation of all the time variable corrections applied to SSH and the range (atmospheric corrections and SSB). It can be seen that dry troposphere introduces the greatest error while the tides have the largest standard-deviations.

Corrections	Mean(cm)	Time variable deep ocean (std dev) (cm)	Time variable Coastal (std dev) (cm)
Dry troposphere	231	0-2	0-2
Wet troposphere	16	5-6	5-8
Ionosphere	8	2-5	2-5
Sea state bias	5	1-4	2-5
Tides	-0-2	0-80	0-500
Dynamic atmosphere	-0-2	5-15	5-15

Table 1 : Typical values of the mean and standard deviation of all the time variable corrections applied to SSH [Vignudelli et al., 2011].

In this document, the best altimeter standards needed to process these altimeter data are described below.

The ocean covers a wide and varied range of applications, which raise a large number of issues. Two examples of this are: Sea State Bias correction for SAR altimetry in the coastal zone; improved tidal corrections in the Arctic Ocean. These are areas of research that require significant investments and sustained research effort over a number of years.

6.2.2. Wet troposphere

The initial aim of this algorithm was to provide the wet tropospheric correction in the coastal zone, where the MWR measurements become invalid to land contamination in the radiometer footprint. In the present implementation the WTC is provided globally for all altimeter ocean measurements.

Whenever an MWR measurement is considered valid, the correction equals the MWR-based wet path delay. For every ocean point along the altimeter ground track for which the MWR-based WTC has been considered invalid according to a set of criteria, a new estimate is obtained along with its associated error. These include coastal points, but also high latitudes. Therefore, apart from land contamination, rain and ice contamination are also spotted and corrected.



From these grids, data were selected as follows (Fig. 5.1): over ocean all points are selected; over land only points up to 30 km from the coast and with an orthometric height < 500 m. The reason for using more ocean than land data is because we wish to reduce the influence of land data in the estimation to the minimum, but at the same time to warrant that the majority of the estimation points will have available ECMWF data for the computation.

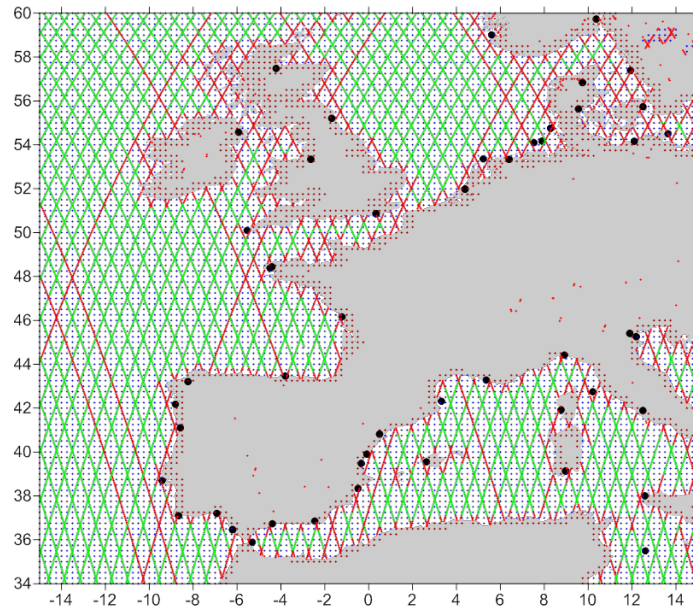


Figure 6.12 : Location of all data sets selected for the GPD computation: **blue** - ECMWF grid points over ocean; **brown** ECMWF grid points over land up to 30 km from the coast; **green** - Envisat ground track points with valid MWR data; **red** - Envisat points with invalid MWR data; **black** - GNSS stations.

The algorithm ensures the continuity and consistency of the correction in the open ocean / coastal transition zone.

Model wet tropospheric correction is computed at the altimeter time-tag from the interpolation of 2 meteorological fields that surround the altimeter time-tag. A wet tropospheric correction must be added (negative value) to the instrument range to correct this range measurement for wet tropospheric range delays of the radar pulse.

GNSS-derived Path Delay (GPD) algorithm: The GPD algorithm is based on the combination of wet path delays (PD) from three data types: Wet PD derived at a network of coastal GNSS (Global Navigation Satellite System) stations; wet PD from valid microwave radiometer (MWR) measurements at the nearby points; tropospheric delays from the European Centre for Medium-range Weather Forecasts (ECMWF) model. At each altimeter point with an invalid MWR value, the wet tropospheric correction is estimated, along with the associated mapping error, using a linear space-time objective analysis technique that takes into account the spatial and temporal variability of the wet path delay field and the accuracy of each data set used.

Mission applicability : Envisat (and any other altimetric mission with an onboard MWR, after adequate algorithm tuning)

The GPD algorithm was designed to compute the WTC on ocean measurements. Initially, the computation was restricted to coastal areas, where a set of GNSS inland stations can be found. In the present implementation an estimate is obtained for every ocean point along the altimeter ground track for which the WTC computed from MWR measurements has been considered invalid. The validity of an MWR measurement is set by an MWR rejection flag (MWR_REJ) according to the following criteria (for Envisat, Figure 6.13):

- MWR_REJ = 1 - if the rad_surf_type flag is 1 (land contamination)
- MWR_REJ = 2 - if the rad_qual_interp_flag is \neq 0 (land contamination)



- MWR_REJ = 3 - if the ice_flag is 1 (ice contamination)
- MWR_REJ = 4 - if the MWR WTC is ≥ 0 or < 0.5 m (rain or ice contamination, or instrument failure)
- MWR_REJ = 5 - if the absolute value of the difference between the MWR and ECMWF WTC is ≥ 10 cm (rain or ice contamination)

Figure 6.13 and Figure 6.14 illustrate the application of the algorithm to Envisat cycle 58.

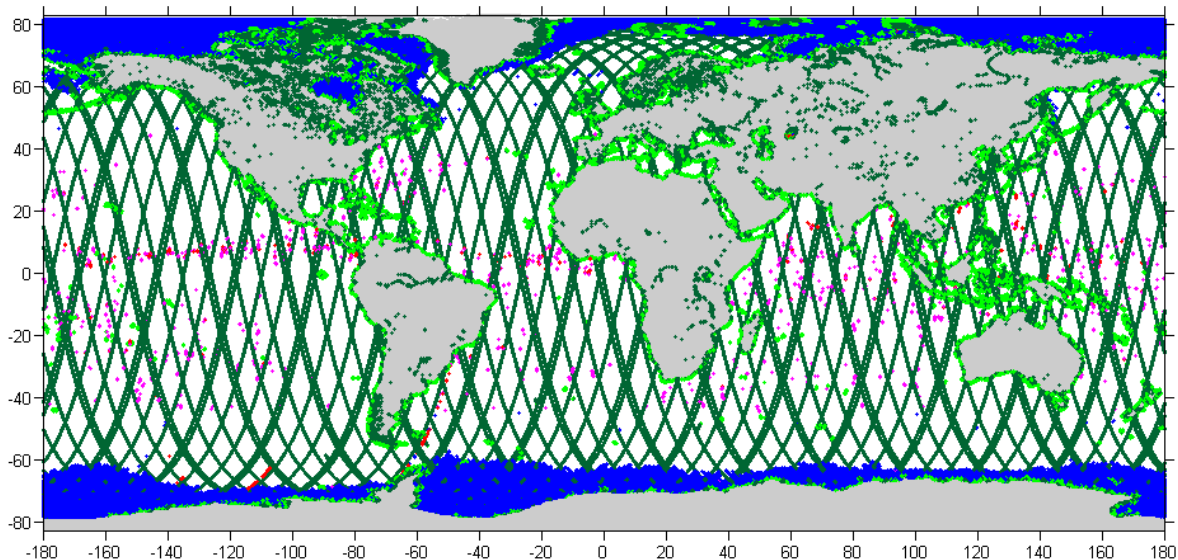


Figure 6.13 : Location of Envisat cycle 58 ground track points selected for the GPD computation. Only points with invalid MWR data ($MWR_REJ \neq 0$) are shown. Dark green: points with $MWR_REJ=1$; Light green: points with $MWR_REJ=2$; Blue: points with $MWR_REJ=3$; Red: points with $MWR_REJ=4$; Pink: points with $MWR_REJ=5$ (see text for details).

Accuracy

Fig. 5.3 illustrates the formal error associated with each GPD estimate for Envisat cycle 58. Several configurations can be found that allow the estimation of the wet delays within 1 cm formal error: points at distances $< \sim 50$ km from a GNSS station, points for which there are valid MWR measurements within a distance $< \sim 50$ km or passes with an associated time very close in time to one ECMWF grid.

Considering that each output is a combination of all available observations, in the worst case the estimation is solely based on ECMWF-derived values. In this case, when the time difference between the estimated point and the closest ECMWF grid is large (up to 3h), the corresponding formal errors will be large as it can be observed along some tracks in Figure 6.13.

Concerning the availability of valid MWR measurements, the worst cases take place when an isolated segment with all points having invalid MWR measurements occurs (usually when the track is parallel to the coastline, where a contaminated segment of several hundreds of kilometers length may occur).

Considering the GNSS-derived path delays, various regions can be identified in Figure 6.12, e.g. around European coastlines, where relatively dense networks of coastal stations can be found. However, there are many regions, particularly in the African coast, without available GNSS stations for distances of several hundreds of kilometers. For this purpose, a densification of the network of coastal GNSS stations would be desirable, with a station approximately every 100 km.

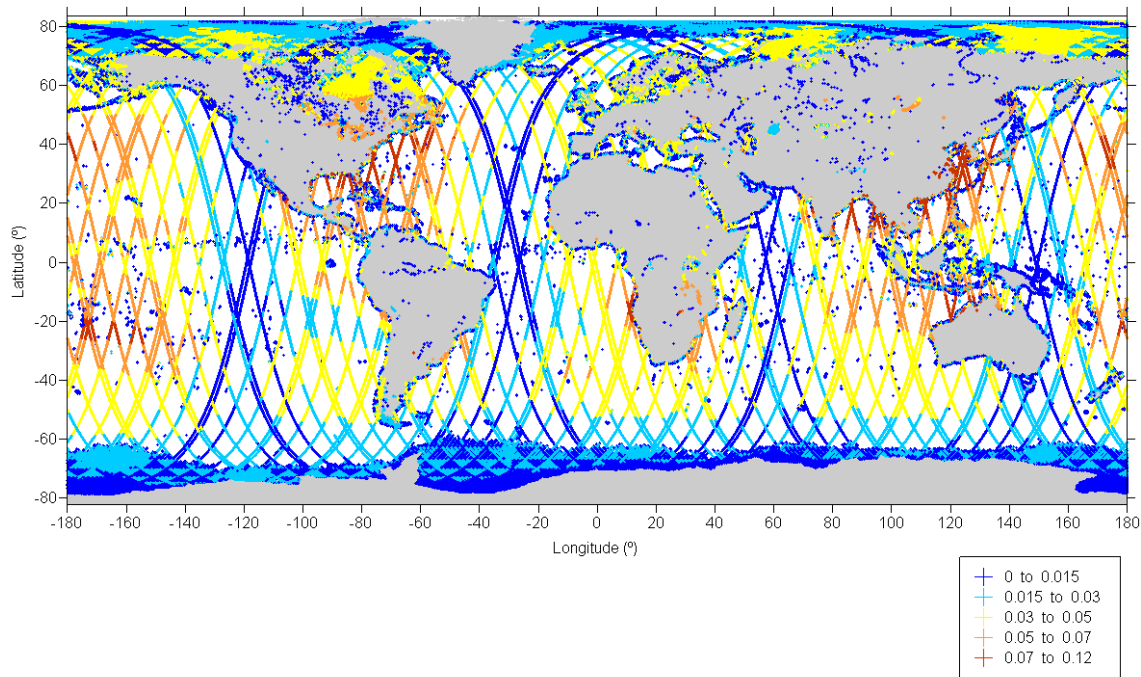


Figure 6.14 : Formal error (in metres) for EnviSat cycle 58.

6.2.3. Dry troposphere

ECMWF operational Model dry tropospheric correction is computed at the altimeter time-tag from the interpolation of 2 meteorological fields that surround the altimeter time-tag. A dry tropospheric correction must be added (negative value) to the instrument range to correct this range measurement for dry tropospheric range delays of the radar pulse.

The surface pressure and the mean sea surface pressure at the altimeter measurement are obtained by linear interpolation in time between two consecutive (6 hours apart) ECMWF model data files, and by bilinear interpolation in space from the four nearby model grid values (excepted for the mean sea surface pressure). The ECMWF model grid is quasi regular in latitude and non-regular in longitude (the number of grid points in longitude increases towards lower latitudes). If the surface type of the altimeter measurement is set to “open ocean or semi-enclosed seas”, only grid points having negative altitude are used in the interpolation (to avoid wrong tropospheric correction to be computed over ocean due to a grid point over high land altitude). If no such grid points with negative altitude are found, then the four grid points having positive altitude are used. If the altimeter measurement is set to “enclosed seas or lakes”, “continental ice”, or “land”, all grid points are used in the interpolation, whatever their altitude is.

The accuracy of the dry tropospheric correction primarily depends on the accuracy of the surface pressure. The best accuracy for surface pressure is achieved for analyzed fields. Typical errors vary from 1 hPa in northern Atlantic to more than 10 hPa in southern Pacific. A 1 hPa error on pressure translates to a 2 mm error on the dry tropospheric correction. The error introduced by space and time interpolation under the satellite track is probably small compared with the intrinsic inaccuracy of the surface pressure. For land surfaces, additional error is induced by the calculation of the surface pressure from the upper level pressure, due to assumptions on the mean virtual temperature of the atmospheric layer between the surface and the first upper level above the ground surface, and due to inaccurate knowledge of the TerrainBase digital elevation model (DEM) used for computing the altitude of the grid points above mean sea level. This additional error may be as large as the intrinsic error of the upper level pressure.



6.2.1. Ionospheric correction

To compute the ionosphere correction (based on a GPS climatology for the total electron content in the ionosphere) of the sea surface topography at the altimeter time tag and location.

the ionospheric correction: GIM reprocessed or current model. GIM ionospheric correction from NASA/JPL. An ionospheric correction must be added (negative value) to the instrument range to correct this range measurement for ionospheric range delays of the radar pulse.

6.2.2. Dynamical atmospheric correction

The Dynamical atmospheric correction is a combination of high frequencies of a barotropic model forced by pressure and wind (MOG2D model: *Carrère and Lyard 2003; SWT New Orleans 2002*) and the low frequencies of the inverse barometer.

the dynamical atmospheric correction: Also known as high frequency fluctuations of the sea surface topography which contains the combined atmospheric corrections (from MOG2D model + inverse barometer)

The DAC is based on a global barotropic model (MOG2D), which has inherent errors due to the physic approximations, the grid size, the forcing fields, the bathymetry errors ... Model outputs have been extensively compared to in situ data (tidal gauge, noted TGs; *Carrère et Lyard 2003; Carrère, 2013*): the model represents about 80 % of the high frequency variability and it allows reducing the TG variance by more than 50% if compared to the static IB; at low latitudes (between +/- 30°) the model is less efficient (gain of 10-20%) due to the dominance of the baroclinic signal, however signal is very weak in these regions. The residual variance of the temporal series corrected from the DAC correction, gives an estimation of the global error of this component, including: modelling errors (bathymetry, mesh resolution, forcing errors ...), omissions errors, due to the lack of baroclinic physic for example. This global error is less than 10 % at high latitudes, and between 40-80 % at low latitudes; if looking at cm², the residual variance is lower than 2 cm² in the intertropical region, where the variability at high frequencies is very weak, and about 5-10 cm² near the coasts (locally more than 100 cm²), where the high frequency variability is strong. Concerning barotropic velocities, the error distribution is mainly localized in coastal margin and in cape-like areas; in deeper regions this error is negligible.

6.2.3. Ocean tide

The tide model computes the tide correction at satellites location and date using GOT4v8 wave tide files of amplitude and phase.

Ocean tide: Geocentric ocean tide height (solution 1): GOT4.8 from GSFC : Includes the loading tide and equilibrium long-period ocean tide height. The permanent tide (zero frequency) is not included in this parameter because it is included in the geoid and mean sea surface. Fes04 model or GOT model

A typical value for deep ocean tide model error is a 1 cm error (*Lyard et al. 2006; Ray, 2011; Carrère et al, 2012; Cancet et al.2012*). This error will likely be reduced while improving the in situ comparison dataset (work being done by R. Ray, personal communication 2013). In shallow water this error is higher due to higher modelling and omission errors: the modelling error includes bathymetry error, mesh resolution, and hydrodynamic approximations error, and the omission error is due to the lack of non linear waves in most of models. The global rms difference with a 179-shallow-waters database is about 10 cm (*Ray, 2011*), but it can reach several tens of cm if compared to a more complete and coastal database (*Cancet et al, 2012; Carrère et al. 2012*):



between 18-36 cm error for M2 wave if compared to a coastal dataset, and between 20-50 cm for a shelf database (extended dataset if compared to R. Ray's one). Most recent tidal model FES2012 shows a smaller error of about 6 cm for M2, on those both databases.

6.2.4. Solid Earth tide

Solid Earth tide: Solid earth tide height is calculated using Cartwright and Taylor tables and consisting of the second and third degree constituents. The permanent tide (zero frequency) is not included. From Cartwright and Edden [1973] Corrected tables of tidal harmonics - J. Geophys. J. R. Astr. Soc., 33, 253-264.

6.2.5. Pole tide

Pole tide: Computed from Wahr [1985] Deformation of the Earth induced by polar motion - J. Geophys. Res. (Solid Earth), 90, 9363-9368.

6.2.6. Mean Sea Surface

The DTU10 MSS has been selected in order to favour the Arctic Ocean which is an area of main interest for climate studies (Andersen, 2009). On the other hand, the use of the DTU10 MSS instead of CNES/CLS 2011 MSS (mean sea surface height above reference ellipsoid from CLS/CNES) reduces the SLA performances in the open ocean which could have an impact on mesoscale applications. The mean sea surface is the displacement of the sea surface relative to a mathematical model of the earth and it closely follows the geoid. Amplitudes range between +/- 100 meters. DTU10 Ocean wide Mean Sea Surface height (relative to the Ellipsoid) has been mapped with a resolution of 1 minute by 1 minute corresponding to 2 minute by 2 minute resolution at Equator (<ftp.spacecenter.dk/pub/MSS>)

The height of the MSS is computed at the altimeter measurement using a squared window of NxN MSS grid points (typically N = 6) centered on the altimeter point. Spline functions are calculated within the window as function of grid point latitude for each MSS column. Each of these spline functions is evaluated at the altimeter latitude. The resulting values are then used for calculating a spline function of grid point longitude. The height of the MSS is derived by evaluating the spline at the altimeter longitude. When one MSS grid point has a default value (grid point over land), then a lower N value is tried. If spline interpolation fails (because N < 4), then bilinear interpolation is performed. An offset may be added to the computed height of the MSS.

A MSS flag is also derived. It addresses the quality of the interpolation by providing the number of grid cells used during the spline (or bilinear) interpolation process. The accuracy is also provided at the location of the measurement by the MSS accuracy map (calibrated formal errors) using a bilinear interpolation.

6.2.7. Sea Sate Bias

The sea state bias (SSB) is the difference between the apparent sea level as "seen" by an altimeter and the actual mean sea level.

This correction is interpolated on 1Hz measurements from a 2-dimensional table which contains [No-parametric 2007 (Labroue)]:

- altimetric Ku waves
- altimetric Ku wind



Note that the sea-surface bias (electromagnetic sea-surface bias) has not been considered in the corrections since no SSB solutions are available for both RDSAR and SAR methods at this stage. In this way the same corrections are applied for the RDSAR and SAR sea level measurements.

6.3. SAR mode coverage

User expectations for enhanced Altimeter SAR coverage are evolving based on the recent (2012) findings from the CryoSat mission operating in SAR mode over the open ocean, highlighting extremely promising benefits that could be expected from the Sentinel-3 SAR altimeter operating in SAR mode over the entire ocean.

The selection of test areas for the validation of Cryosat-2 SAR mode over the open and coastal ocean is determined by:

- the data need given the specific objectives of the validation (i.e. location, duration)
- the availability of Cryosat-2 data in the requisite mode for the requisite location and the requisite duration to make validation possible
- the availability of Cryosat-2 data processed with the appropriate processor baseline

The availability of Cryosat-2 data in different modes (LRM, SAR and SARIN) is determined by the data acquisition mode mask.

Figure 6.15 shows some of the main versions of the mask, together with the approximate periods covered by each version of the mask in the right-hand column. As can be seen in

Figure 6.15, the mask evolved significantly during the mission lifetime.

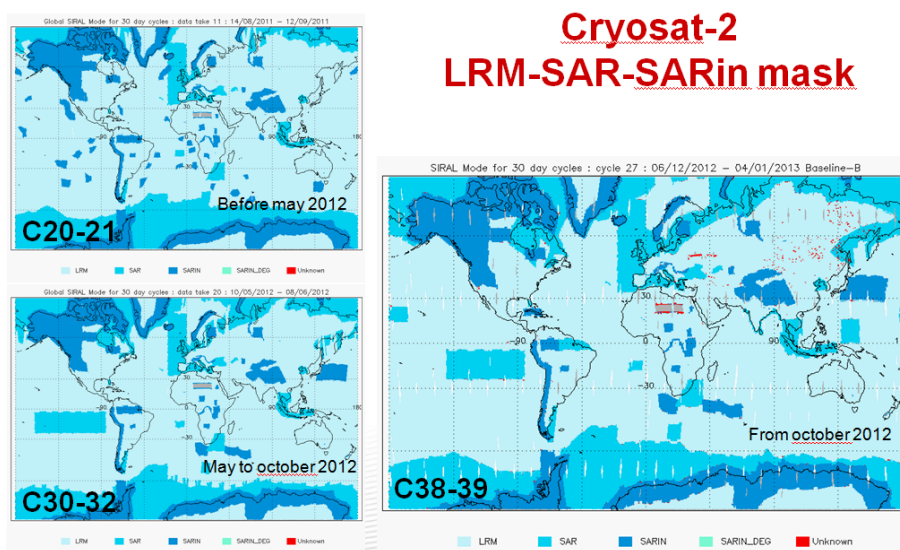


Figure 6.15 : CS-2 LRM/SAR/SARin mode mask for 3 different periods



7. References

- [Amarouche et al., 2004]: L. Amarouche, P. Thibaut, O.Z. Zanife, J.-P. Dumont, P. Vincent and N. Steunou, “Improving the Jason-1 ground retracking to better account for attitude effects”, *marine Geodesy*, Vol. 27, pp.171-197, 2004.
- [Andersen et al., 2009]: O. B. Andersen and P. Knudsen, “DNSCO8 mean sea surface and mean dynamic topography models”, *J. Geophys. Res.*, 114, C11001, doi:10.1029/2008JC005179.
- [Boy et al., 2012]: F. Boy, T. Moreau, J-D. Desjonquères, S. Labroue, N. Picot, J-C. Poisson and P. Thibaut, “Cryosat Processing Prototype, LRM and SAR Processing”, presented at the 2012 Ocean Surface Topography Science Team Meeting. Available online: http://www.aviso.oceanobs.com/fileadmin/documents/OSTST/2012/oral/02_friday_28/02_instr_processing_II/02_IP2_Boy.pdf
- [Boy et al., 2013]: F. Boy and T. Moreau, “Algorithm Theoretical Basis Document (ATBD) of the CPP SAR numerical retracker for oceans”, S3A-NT-SRAL-00099-CNES, June 2013.
- [Cancet et al., 2012]: Cancet, M. and J. Lamouroux, “Modèle de marée FES2012 - tâche 4”, NOV-3918-NT-12304_v2.0.pdf, 10/2012.
- [Carrère et al., 2003]: L. Carrère and F. Lyard, “Modeling the barotropic response of the global ocean to atmospheric wind and pressure forcing - comparison with observations”, *Geophysical Research Letters*, Vol. 30, NO 6, 1275, doi:10.1029/2002GL016473, 2003
- [Carrère et al., 2012]: L. Carrère, F. Lyard, M. Cancet, A. Guillot, L. Roblou, “FES 2012: a new global tidal model taking advantage of nearly 20 years of altimetry”, *Proceeding of the 20 Years of Progress in Radar Altimetry Symposium*, Venice, Italy, 2012.
- [Clarizia et al., 2012] M.P. Clarizia, D. Cotton and E. Gil-Roldan, “Cryosat Plus for Oceans: User Consultation”, poster presented at the 6th Coastal Altimetry Workshop in Riva del Garda, Italy, and Ocean Surface Topography Science Team (OSTST) meeting in Venice, Italy (Sept. 2012).
- [Cotton et al., 2008]: D. Cotton, O. Andersen, P. Cipollini, C. Gommenginger, G. Quartly, C. Martin, J. Marquez, L. Moreno, “Development of SAR Altimetry Mode Studies and Applications over Ocean, Coastal Zones and Inland Water (SAMOSA): State of Art Assessment”, Report for ESA/ESRIN Contract No. AO/1-5254/06/I-LG, available at <http://www.satoc.eu/projects/samosa/docs/SAMOSA-TN01-V1.0full.pdf>
- [CryoSat DQSS, 2013]: “CryoSat Data Quality Status Summary”, ESA report ESRIN-EOP-GQ, CS-TN-ESA-GS-808 Version 6, 15 July 2013, 23 pp. Available from ESA website: <https://earth.esa.int/web/guest/missions/cryosat/product-status>
- [Desjonquères et al., 2012]: J.D. Desjonquères, F. Boy and N. Picot, “Altimeter SAR data over ocean - CNES processing strategy and continuity with LRM data”, poster at the 2012 American Geophysical Union Meeting.
- [Dufau et al., 2008]: C. Dufau and C. Martin-Puig., “User Requirements for COASTALT and PISTACH”, summary presentation given at the 2nd Coastal Altimetry Workshop 2008, Pisa, ITALY. Available at <http://www.coastalt.eu/sites/coastalt.eu/files/pisaworkshop08/pres/01-PISTACH-COASTALT-CAW-V4-CMP.pdf>
- [Dufau et al., 2011]: C. Dufau, C. Martin-Puig, and L. Moreno, “User requirements in the coastal ocean for satellite altimetry”, in *Coastal Altimetry*, Eds S. Vignudelli, A. Kostianoy. P. Cipollini, J. Benveniste, Springer, 2011.
- [ECMWF, 2009]: ECMWF (2009) <http://www.ecmwf.int/products/catalogue/pseta.html>
- [Fernandes et al., 2010]: M.J. Fernandes, C. Lázaro, A.L. Nunes, N. Pires, L. Bastos, V.B. Mendes, “GNSS-derived Path Delay: an approach to compute the wet tropospheric correction for coastal altimetry”, *IEEE Geosci. Rem. Sens Lett.*, 7(3): 596–600, 2010
- [Fernandes et al., 2012]: M.J. Fernandes, N. Pires, C. Lázaro, A.L. Nunes, “Tropospheric Delays from GNSS for Application in Coastal Altimetry”, *Advances in Space Research*, Vol. 51(8). doi:10.1016/j.asr.2012.04.025, 2012.



[Galín et al., 2013]: N. Galín, D. Wingham, R. Cullen, R. Francis, I. Lawrence, “*Measuring the Pitch of CryoSat-2, Using the SAR Mode of the SIRAL Altimeter*”, Poster presented at the Living Planet Symposium in Edinburgh, UK, 9-13 Sept. 2013.

[Gommenginger et al., 2011]: C. Gommenginger, C. Martin-Puig, S. Dinardo, D. Cotton, M. Srokosz, and J. Benveniste, “*Improved altimetric accuracy of SAR altimeters over ocean: Observational evidence from Cryosat-2 SAR and Jason-2*”, Ocean Surface Topography Science Team 2011, San Diego, 19-21 Oct. 2011, <http://www.avisioceanobs.com/en/courses/sci-teams/ostst-2011.html>

[Gommenginger et al., 2012]: C. Gommenginger, P. Cipollini, D. Cotton, S. Dinardo, and J. Benveniste, “*Finer, Better, Closer: Advanced capabilities of SAR altimetry in the open ocean and the coastal zone*”, Ocean Surface Topography Science Team 2012, Venice-Lido, Italy, 22-29 Sept. 2012, <http://www.avisioceanobs.com/en/courses/sci-teams/ostst-2012.html>

[Halimi, 2013]: A. Halimi, “*From conventional to delay/Doppler altimetry*”, PhD Thesis, University Toulouse, Oct. 2013.

[Jensen, 1999]: J.R. Jensen, “*Radar altimeter gate tracking: Theory and extension*”, IEEE Trans. Geosci. Rem. Sens., 37 (2), 651-658, 1999.

[Lyard et al., 2006]: Lyard, F., et al. (2006), “*Modelling the global ocean tides: a modern insight from FES2004*”, Ocean Dynamics, 56, 394-415, 2006.

[Moreno et al., 2008]: L. Moreno and C. Martin-Puig, “*COASTALT Report on User Requirements for Coastal Altimetry Products*”, ESA/ESRIN Contract No. 21201/08/I-LG, available at <http://www.coastalt.eu/files/results/COASTALT-WP1-D12-final-red.pdf>

[Phalippou et al., 2007]: L. Phalippou and V. Enjolras, “*Re-tracking of SAR altimeter ocean power-waveforms and related accuracies of the retrieved sea surface height, significant wave height and wind speed*”, Igarss: 2007 IEEE International Geoscience and Remote Sensing Symposium, Vols 1-12, 3533-3536, 2007.

[Phalippou et al., 2011]: L. Phalippou and F. Demeestere, “*Optimal retracking of SAR altimeter echoes over open ocean: Theory versus results from SIRAL2 data*”, Ocean Surface Topography Science Team 2011, San Diego, 19-21 Oct 2011, <http://www.avisioceanobs.com/en/courses/sci-teams/ostst-2011.html>

[Phalippou et al., 2012]: L. Phalippou, E. Caubet, F. Demeestere, J. Richard, L. Rys, M. Deschaux-Beaume, R. Francis, and R. Cullen, “*Reaching sub-centimeter range noise on Jason-CS with the Poseidon-4 continuous SAR interleaved mode*”, In Ocean Surface Topography Science Team Meeting, Venice, Italy, Oct. 2012, , <http://www.avisioceanobs.com/en/courses/sci-teams/ostst-2012.html>

[Ray et al., 2013]: Ray, R.D. (2013), “*Precise comparisons of bottom-pressure and altimetric ocean tides*”, submitted to JGR-Oceans, 2013.

[Smith et al., 2013]: W.H.F. Smith and R. Scharroo, “*Retracking range, SWH, sigma-naught, and attitude in CryoSat conventional ocean data*”, In proceedings of Ocean Surface Topography Science Team Meeting San Diego, October 19-21, 2011.

[Thibaut et al., 2012]: P. Thibaut, T. Moreau, F. Boy and N. Picot, “*Coastal Altimetry : Evolution of measurement and retracking problems when switching from conventional (Ku, Ka) to SAR altimetry*”, presented at the 2012 Coastal Meeting.

[Thibaut et al., 2013]: P. Thibaut, G. Dibarboure, J. Poisson, S.Labroue, C.Dufau, Y. Lasne, F. Boy, J.D.Desjonqueres and N. Picot, “*Investigating short wavelengths correlated errors on low-resolution mode altimetry*”, presented at the 2013 OSTST Meeting, Boulder, USA.

[Thibaut et al., 2013b]: P. Thibaut, Y.Lasne, T.Moreau, J. Poisson, F. Boy and N. Picot, “*LRM (Ku, Ka) and delay/doppler (Ku) waveform processing in coastal zones*”, presented at the 2013 Coastal Meeting, Boulder, USA.

[Vignudelli et al., 2011]: S. Vignudelli, A. G. Kostianoy, P. Cipollini, and J. Benveniste. (eds.). Coastal Altimetry. Springer Verlag, Berlin, 2011.